Mineralogical Magazine, December 2015, Vol. 79(7), pp. 1675–1709

Frontiers in Theoretical Mineralogy

Generating functions for stoichiometry and structure of single- and double-layer sheet-silicates

Frank C. Hawthorne*

Department of Geological Sciences, University of Manitoba, Winnipeg, Manitoba R3T 2N2, Canada

[*Received 16 April 2015; Accepted 12 October 2015; Associate Editor: M. Welch*]

ABSTRACT

Two-dimensional nets may be used to generate the stoichiometry and structure of single-layer and double-layer sheet-silicate minerals. Many sheet-silicate minerals are based on the 3-connected plane nets 6^3, 4.8^2, $(4.6.8)_2(6.8^2)_1$ and $(5^2.8)_1(5.8^2)_1$, and some more complicated nets, e.g. $(5.6.7)_4(5.7^2)_1(6^2.7)_1$, $(4.12^2)_2(4^2.12)_1$, $(5^2.8)_1(5.6^2)_1(5.6.8)_2(6^2.8)_1$, have one or two representative structures. Many complicated sheet-silicate minerals are based on sheets of 2-, 3- and 4-connected tetrahedra that may be developed from 3- and 4-connected plane nets by a series of oikodoméic operations on 3- or 4-connected nets that change the topology of the parent net. There are three classes of oikodoméic operations: (1) insertion of 2- and 3-connected vertices into 3- and 4-connected plane nets; (2,3) replication of single-layer sheets by topological mirror or two-fold-rotation operators, and condensation of the resulting two single-layer sheets to form double-layer sheets. The topological aspects of these sheet structures may be described by functions that express stoichiometry in terms of tetrahedron connectivities (formula-generating functions) and functions that associate these formula-generating functions with specific two-dimensional nets. Using these functions, we may generate formulae and structural arrangements of single-layer and double-layer silicate structures with specific local and long-range topological features.

Keywords: sheet-silicate minerals, bond topology, formula-generating function, structure connectivity, structure-generating function, structure prediction.

Introduction

The relation between chemical composition and atomic arrangement is central to the science of Crystallography, and the main aim of Crystallography is to derive atomic arrangements for known chemical compositions. If one has an atomic arrangement, it is generally trivial to derive the chemical composition: one counts the number of atoms in the unit cell and reduces the resulting chemical formula to a (usually) irreducible form. If one has a chemical composition, to derive an atomic arrangement (without doing an experiment) is usually difficult to impossible. Various methods are available to attempt to find such atomic arrangements for a particular chemical composition, but they are restricted to simple compounds and require very specific boundary conditions. Thus, I suggest that such methods will not be successful in deriving the structure of, for example, veblenite: $K_2\square_2Na(Fe^{2+}_5Fe^{3+}_4Mn_7\square)Nb_3Ti(Si_2O_7)_2(Si_8O_{22})_2O_6(OH)_{10}(H_2O)_3$ (Cámara *et al.*, 2013), let alone predicting its existence as a chemical compound.

Information on structural arrangement is contained in chemical formulae, and we are aware of this information for simple structures, particularly for oxysalt minerals. This information may be exact: For example, $ABSiO_4$ has isolated (SiO_4) tetrahedra; or it may be qualitative: for example, $ABSi_2O_6$ probably has single chains of (SiO_4) tetrahedra; as the degree of connectivity of the tetrahedra changes, so does the corresponding formula. However, this connection is only qualitative, and there are many examples for which our intuition may be wrong. For example, **dmisteinbergite** (Chesnokov *et al.*, 1990) has the formula

* E-mail: frank_hawthorne@umanitoba.ca
DOI: 10.1180/minmag.2015.079.7.17

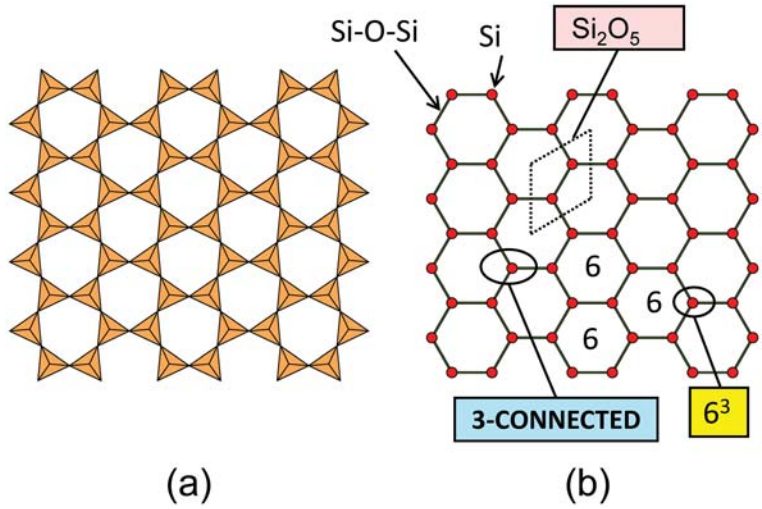

FIG. 1. (*a*) The $[T_2O_5]$ sheet in mica; (*b*) the $(6^3)_2$ net, with vertices shown as red circles and edges shown as green lines; the unit cell is shown by dotted lines.

$Ca[Al_2Si_2O_8]$, i.e. $Ca[TO_2]_4$, suggesting that it is a framework silicate, whereas it is a sheet silicate (Takeuchi and Donnay, 1959). The relation between stoichiometry and structural arrangement has rarely been examined rigorously (although see Hawthorne, 2012). I shall do so here for minerals containing one- and two-layer sheets of cation-centred tetrahedra with the central cation $T = Si^{4+}$, Al^{3+}, Fe^{3+}, B^{3+}, Be^{2+}, Zn^{2+} and Mg^{2+}; for simplicity of expression, I will refer to these structures as sheet silicates, and they are required to contain Si^{4+} as an essential constituent.

Nomenclature

Our focus here is the structure of sheet-silicate minerals, and I will use the term *sheet silicate* rather than the term *phyllosilicate.* When I refer to a ´silicate sheet', let it be understood that the sheet must contain Si^{4+} but it also may contain other tetrahedrally coordinated cations as stated above. Furthermore, I will generally refer to a tetrahedron by its central cation: thus the expression ´Si tetrahedron' represents an $(SiO_4)^{4-}$ tetrahedron, and a ´T tetrahedron' represents a $(TO_4)^{n-}$ tetrahedron where T is one or more unspecified tetrahedrally coordinated cations.

Liebau (1985) divided silicate sheets into *single-layer sheets* and *double-layer sheets*, where double-layer sheets were defined as consisting of a condensation of two single-layer sheets through a mirror plane (or pseudo-mirror plane) parallel to the sheet. This mirror operation is analogous to the sigma operation used in the theoretical construction of framework silicates (e.g. Smith, 1988). I will use this division of *single-layer sheets* and *double-layer sheets* here, but with regard to the condensation of a single-layer sheet to a double-layer sheet, I will not restrict the condensation to a mirror operation. There are three triple-layer silicate minerals known (**gunterblassite**, $(K,Ca)_{3-x}Fe[(Si,Al)_{13}O_{25}(OH,O)_4](H_2O)_7$, Chukanov *et al*., 2012; Rastsvataeva *et al*., 2012; **umbrianite**, $K_7Na_2Ca_2[Al_3Si_{10}O_{29}]F_2Cl_2$, Sharygin *et al*., 2013; **hillesheimite**, $(K,Ca,\square)_2(Mg,Fe,Ca,\square)_2[(Si,Al)_{13}O_{23}(OH)_6](OH).8H_2O$, Chukanov *et al*., 2013). I will not consider triple-layer sheets at this time, but the extension of this approach to triple-layer sheets is straightforward.

Nets and polymerization of tetrahedra

The polymerization of tetrahedra is commonly described in terms of one-, two- and three-dimensional nets in which the vertices of the net are occupied by tetrahedra, and the edges of the net represent linkages between tetrahedra. The relation between the sheet of tetrahedra in the mica structure and its corresponding net is shown in Fig. 1. Each tetrahedron in the mica sheet (Fig. 1*a*) is represented by a vertex (red circle) in the corresponding net (Fig. 1*b*). Linkage between tetrahedra is shown by edges between vertices (green lines in Fig. 1*b*). Each

https://doi.org/10.1180/minmag.2015.079.7.17 Published online by Cambridge University Press

vertex has three incident edges and hence all vertices are 3-connected. Each vertex is surrounded by three hexagons and is given the symbol 6^3, and all vertices are identical. A net is labelled by the types and relative numbers of the vertices it contains; there is one type of vertex in the net shown in Fig. 1*b*, and this net is designated the 6^3 net. The unit cell of the net is shown by the dotted black lines and has the content $[Si_2O_5]$, or more generally $[T_2O_5]$. The conventional net symbol does not carry information on the number of vertices in the unit cell. This may not be a difficulty when dealing with nets such as 6^3, which are simple and well-known, as one is aware of the number of vertices in the unit cell, but this is not the case when dealing with unusual nets with many vertices in the unit cell. As we are relating the connectivity of nets and sheets of tetrahedra to their stoichiometry, the number of vertices in the unit cell of a net is of obvious importance. Moreover, if we colour a net and increase the size of the unit cell (but not the connectivity) of the net, the number of its constituent vertices will change. Hence it is advantageous to denote the number of vertices in the unit cell of a net. I will do this by enclosing the vertex symbols in parentheses and attaching a subscript or subscripts that indicate the number of vertices in the unit cell; thus the symbol for the 6^3 net shown in Fig. 1*b* becomes $(6^3)_2$. Where I wish to refer to the net without specifying the size of the unit cell, I will use the unadorned net symbol, i.e. 6^3.

Nets have been used extensively in the description and theoretical derivation of framework silicates (e.g. Smith, 1977, 1978, 1988; Hawthorne and Smith, 1986*a*,*b*, 1988) and other minerals (e.g. Hawthorne *et al*., 2000; Krivovichev, 2008, 2009) although as far as I am aware, the relation between stoichiometry and structure has not been investigated in any detail. We will use an analogous approach here. Tetrahedra are described as *n*-connected ($n = 0$–4) if they share corners with *n* other tetrahedra. A net is described as *n*-connected if all vertices of that net have *n* edges incident at each vertex. We require that a sheet (and its analogous net) be continuous, that is connected, in two dimensions. Two-dimensional nets with only one type of vertex must contain 3-connected vertices in order to be continuous. Thus we will start our analysis of sheets of tetrahedra by examining plane 3-connected nets, and modifying them by a series of topological building algorithms that add vertices and edges to the parent nets.

A sheet of tetrahedra does not require all its constituent tetrahedra to be 3-connected, and we will introduce other-connected vertices into plane nets in order to reflect this diversity. We will also introduce topological operators in order to generate more complicated double-layer sheets of tetrahedra. The general philosophy of this approach is that the form of the initial (parent) nets and the building algorithms all affect the stoichiometry of the resulting structure, and will provide us with a more rigorous connection between stoichiometry and structure in sheet-silicate minerals.

Three-connected plane nets

There is an infinite number of 3-connected plane nets and we need to select those that are relevant (or potentially relevant) to sheet-silicate minerals; we will start with the more simple of the 3-connected plane nets. There are three regular plane nets (nets that show edge-to-edge connectivity of congruent regular polygons): $(3^6)_1$, $(4^4)_1$ and $(6^3)_2$ but only $(6^3)_2$ is 3-connected (Fig. 1*b*). There are three semi-regular 3-connected plane nets (nets that show edge-to-edge connectivity of regular polygons): $(4.8^2)_4$, $(3.12^2)_6$ and $(4.6.12)_{12}$ (Fig. 2). There are many other 3-connected plane nets containing non-regular polygons. We consider an additional six nets where the polygons defined by the rings of vertices deviate only slightly from regularity and do not exceed ten edges (Figs 3, 4). The resulting ten nets are listed in Table 1 in terms of increasing content of the unit cell.

The three semi-regular 3-connected plane nets $(4.8^2)_4$, $(3.12^2)_6$ and $(4.6.12)_{12}$ are shown in Fig. 2. The net in Fig. 2*a* has two types of rings of vertices, a four-membered ring and an eight-membered ring. There are one four-membered ring and two eight-membered rings incident at each vertex, and the vertex is labelled 4.8^2; there is only one type of vertex in this net, there are four vertices in the unit cell, and the net is the plane net $(4.8^2)_4$. The net in Fig. 2*b* also has two types of rings of vertices, a three-membered ring and a twelve-membered ring. There are one three-membered ring and two twelve-membered rings incident at each vertex, and the vertex is labelled 3.12^2; there is only one type of vertex in this net, there are six vertices in the unit cell, and the net is the plane net $(3.12^2)_6$. The net in Fig. 2*c* has three types of rings of vertices, a four-membered ring, a six-membered ring and a twelve-membered ring. There is one type of each ring incident at each vertex, and the vertex is labelled 4.6.12; there is only one type of vertex in this net, there are twelve vertices in the unit cell, and the net is the plane net $(4.6.12)_{12}$.

https://doi.org/10.1180/minmag.2015.079.7.17 Published online by Cambridge University Press

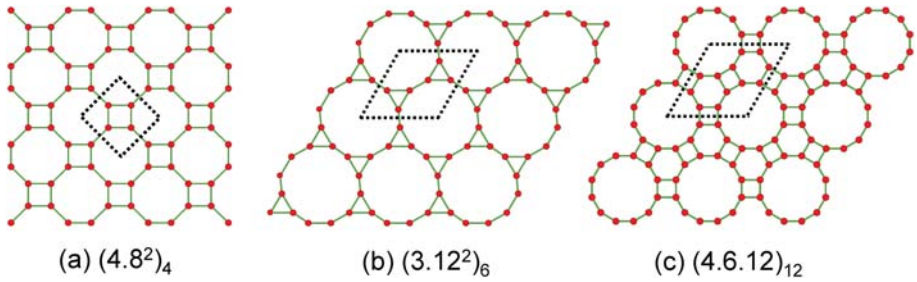

FIG. 2. Three-connected semi-regular plane nets; (*a*) the $(4.8^2)_4$ net; (*b*) the $(3.12^2)_6$ net; (*c*) the $(4.6.12)_{12}$ net; legend as in Fig. 1.

Simple 3-connected plane nets of non-regular polygons are shown in Figs 3 and 4, and a major characteristic of these nets is that they each contain more than one type of vertex. The net in Fig. 3*a* has three types of rings of vertices, a four-membered ring, a six-membered ring and an eight-membered ring. There are two types of vertex: (i) one four-membered ring, one six-membered ring and one eight-membered ring are incident at the vertex 4.6.8, and (ii) one six-membered ring and two eight-membered rings are incident at the vertex 6.8^2. There are twice as many 4.6.8 vertices as 6.8^2 vertices, there are six vertices in the unit cell, and the net is $(4.6.8)_4(6.8^2)_2$. The net in Fig. 3*b* has two types of rings of vertices, a five-membered ring and an eight-membered ring. There are two types of vertex: (i) two five-membered rings and an eight-membered ring are incident at the vertex $5^2.8$, and (ii) one five-membered ring and two 8-membered rings are incident at the vertex 5.8^2. There are twice as many $5^2.8$ vertices as 5.8^2 vertices, there are six vertices in the unit cell, and the net is $(5^2.8)_4(5.8^2)_2$.

The net in Fig. 4*a* has three types of rings of vertices, a four-membered ring, a six-membered ring and a ten-membered ring. There are two types of vertex: (i) one four-membered ring, one six-membered ring and one ten-membered ring are incident at the vertex 4.6.10, and (ii) two six-membered rings and one ten-membered ring are incident at the vertex $6^2.10$. There are four times as many 4.6.10 vertices as $6^2.10$ vertices, there are ten vertices in the unit cell, and the net is $(4.6.10)_8(6^2.10)_2$. The net in Fig. 4*b* has three types of rings of vertices, a three-membered ring, a six-membered ring and an eight-membered ring. There are two types of vertex: (i) one three-membered ring and two eight-membered rings are incident at the vertex 3.8^2, and (ii) one six-membered ring and two eight-membered rings are incident at the vertex 6.8^2. There are equal numbers of 3.8^2 and 6.8^2 vertices, there are twelve vertices in the unit cell, and the net is $(3.8^2)_6(6.8^2)_6$. The net in Fig. 4*c* has three types of rings of vertices, a five-membered ring, a six-membered ring and an eight-membered ring. There are four types of vertex: (i) two five-membered rings and one eight-membered ring are incident at the vertex $5^2.8$; (ii) one five-membered ring and two six-membered rings are incident at the vertex 5.6^2; (iii) one five-membered ring, one six-membered ring and one eight-membered ring are incident at the vertex 5.6.8; and (iv) two six-membered rings and one eight-membered ring are incident at the vertex $6^2.8$. There are equal numbers of $5^2.8$, 5.6^2 and $6^2.8$ vertices and twice as many 5.6.8 vertices, there are twenty vertices in the unit cell, and the net is $(5^2.8)_4(5.6^2)_4(5.6.8)_8(6^2.8)_4$. The net in Fig. 4*d* has three types of rings of vertices, a five-membered ring, a six-membered ring and a seven-membered ring. There are three types of vertex: (i) one five-membered ring, one six-membered ring and one seven-membered ring are incident at the vertex 5.6.7; (ii) one five-membered ring and two seven-membered rings are incident at the vertex 5.7^2; and (iii) two six-membered rings and one seven-membered ring are incident at the vertex $6^2.7$. There are four times as many 5.6.7 vertices as 5.7^2 or $6^2.7$ vertices, there are twenty-four vertices in the unit cell, and the net is $(5.6.7)_{16}(5.7^2)_4(6^2.7)_4$.

u-d strings and the relative orientation of tetrahedra in sheets of tetrahedra

So far, we have been considering the topological characteristics of plane nets in which each vertex represents a tetrahedron. However, a vertex is a point whereas a tetrahedron is a three-dimensional object; a vertex has no orientation relative to the plane of the net, which is not the case for a tetrahedron. For a 3-connected tetrahedron, the

https://doi.org/10.1180/minmag.2015.079.7.17 Published online by Cambridge University Press

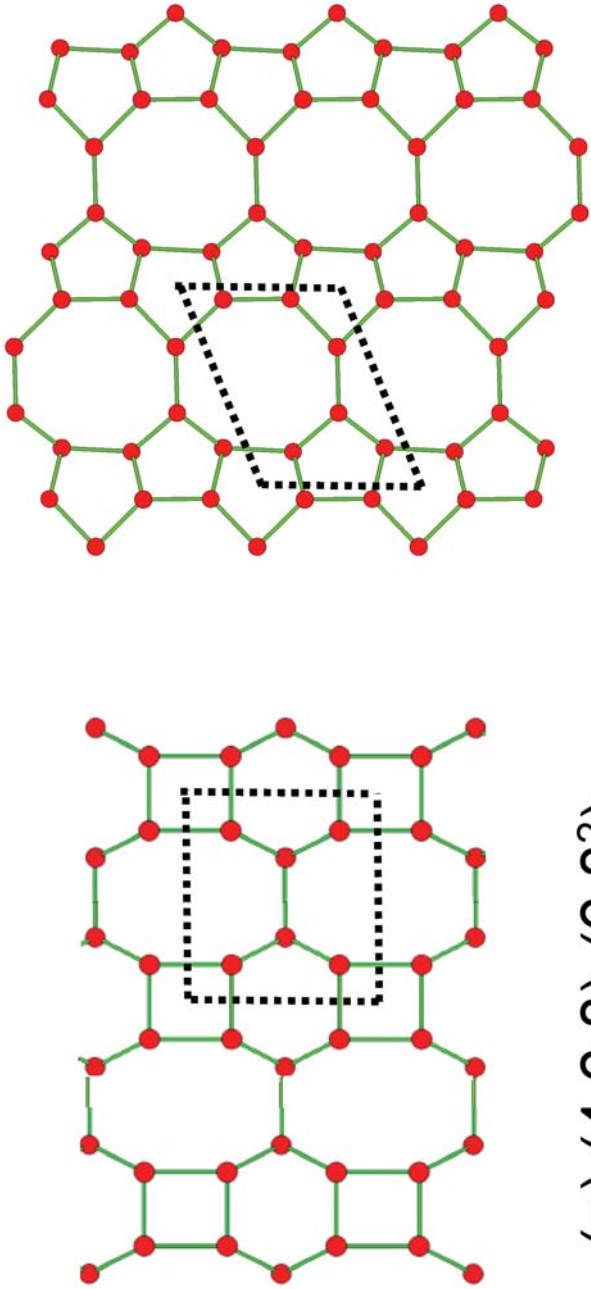

FIG. 3. Three-connected plane nets with six vertices in the unit cell; (*a*) the $(4.6.8)_4(6.8^2)_2$ net; (*b*) the $(5^2.8)_4(5.8^2)_2$ net; legend as in Fig. 1.

https://doi.org/10.1180/minmag.2015.079.7.17 Published online by Cambridge University Press

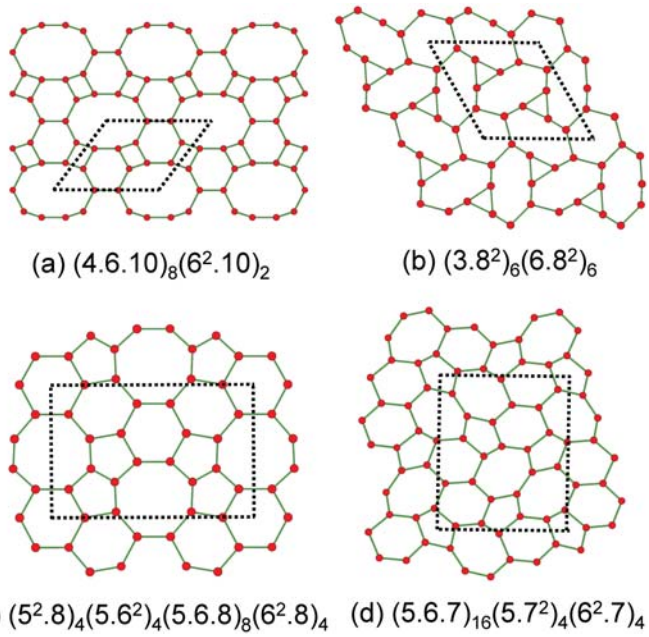

FIG. 4. Some three-connected plane nets with more than six vertices in the unit cell; (*a*) the $(4.6.10)_8(6^2.10)_2$ net; (*b*) the $(3.8^2)_6(6.8^2)_6$ net; (*c*) $(5^2.8)_4(5.6^2)_4(5.6.8)_8(6^2.8)_4$ net; (*d*) the $(5.6.7)_{16}(5.7^2)_4(6^2.7)_4$ net; legend as in Fig. 1.

apical anion (the anion that is [1]-coordinated) may lie on one side of the sheet or the other. When considering only a single tetrahedron, this distinction has no meaning. However, for two or more tetrahedra, the situation is different: the tetrahedra may point in the same direction or the tetrahedra may point in different directions. Figure 5*a* shows tetrahedra at the vertices of the $(6^3)_2$ net, and both Figs 5*a* and 5*b* show that the tetrahedra all point in the same direction, which we will designate as u (up). All six-membered rings are identical in Fig. 5*a*, and we write the attitude of the tetrahedra in this ring as (u^6) (Fig. 5*c*).

Figure 6*a* shows tetrahedra at the vertices of the $(6^3)_8$ net, and both Figs 6*a* and 6*b* show that the tetrahedra point in both directions, u and d (down),

TABLE 1. Simple 3-connected plane nets.*

Number	Symbol	Unit-cell content	Fig.
1	$(6^3)_2$	Si_2O_5	1*b*
2	$(4.8^2)_4$	Si_4O_{10}	2*a*
3	$(3.12^2)_6$	Si_6O_{15}	2*b*
4	$(4.6.8)_4(6.8^2)_2$	Si_6O_{15}	3*a*
5	$(5^2.8)_4(5.8^2)_2$	Si_6O_{15}	3*b*
6	$(4.6.10)_8(6^2.10)_2$	$Si_{10}O_{25}$	4*a*
7	$(4.6.12)_{12}$	$Si_{12}O_{30}$	2*c*
8	$(3.8^2)_6(6.8^2)_6$	$Si_{12}O_{30}$	4*b*
9	$(5^2.8)_4(5.6^2)_4(5.6.8)_8(6^2.8)_4$	$Si_{20}O_{50}$	4*c*
10	$(5.6.7)_{16}(5.7^2)_4(6^2.7)_4$	$Si_{24}O_{60}$	4*d*

*The conventional net symbols (see text) have been augmented by the addition of subscripts that denote the number of vertices in the unit cell.

https://doi.org/10.1180/minmag.2015.079.7.17 Published online by Cambridge University Press

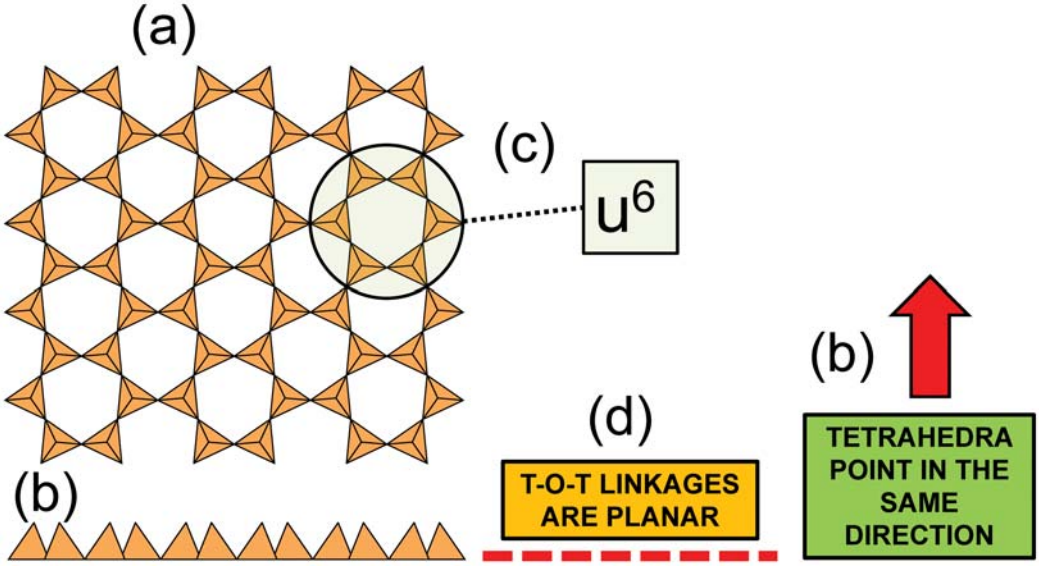

FIG. 5. (*a*) Tetrahedra at the vertices of the 6^3 plane net pointing in the same direction; (*b*) cross-sectional view of the sheet in Fig. 5a; (*c*) all tetrahedra in a six-membered ring point in the same direction (u = up); (*d*) planar arrangement of 3-connected vertices in the sheet.

relative to the plane of the net. There are two distinct six-membered rings in Fig. 6*a*; in one of the rings, all tetrahedra point in the same direction: (u^6) (Fig. 6*c*); in the other ring, tetrahedra point in

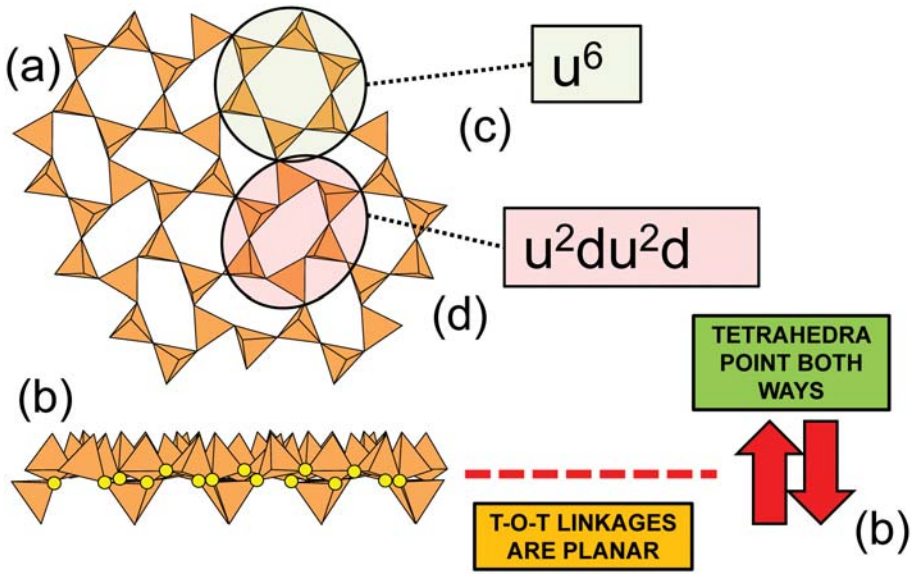

FIG. 6. (*a*) Tetrahedra at the vertices of the 6^3 plane net pointing in different directions; (*b*) cross-sectional view of the sheet in Fig. 6a, note the planar arrangement of 3-connected vertices in the sheet; (*c*) all tetrahedra in a six-membered ring point in the same direction (u = up); (*d*) tetrahedra in a six-membered ring point in different directions (u = up, d = down).

https://doi.org/10.1180/minmag.2015.079.7.17 Published online by Cambridge University Press

different directions: four point up (in the same direction as the tetrahedra in the first ring) and two point down (in the opposite direction to the tetrahedra of the first ring), and the sequence around the ring gives the symbol (u^2du^2d) (Fig. 6*d*). Thus the attitude of the tetrahedra in a sheet may be represented by these u-d strings.

Three-connected plane nets and their unit cells

Inspection of Figs 3 and 4 show that different nets have different unit cells. This is a major factor in the relation between structure and stoichiometry. Figures 7*a*,*b*,*c* show the plane 3-connected nets $(6^3)_2$, $(4.8^2)_4$ and $(4.6.8)_4(6.8^2)_2$, respectively. The contents of the unit cells are $[Si_2O_5]$, $[Si_4O_{10}]$ and $[Si_6O_{15}]$, respectively, and this is commonly reflected in the formulae of the minerals with structures corresponding to these nets. However, this is not necessarily the case. We could write $[Si_4O_{10}]$ as $[Si_2O_5]_2$, but this has the disadvantage of concealing the character of the underlying net. Similarly, the unit cell of a mineral containing a sheet based on the $(6^3)_2$ net can be larger than the unit cell of the underlying net if the non-sheet constituents define a larger unit-cell, and we could write the stoichiometry of the net as $[Si_{2n}O_{5n}]$ where n is a multiple relating the unit cell of the structure to that of the underlying net. However, to do either of these things is to lose structural information from the formula. If we always write the sheet constituents of the mineral in terms of the underlying net, e.g. $[Si_2O_5]_2$ for a structure based on the $(6^3)_4$ net but having a doubled unit-cell relative to that of the $(6^3)_2$ net, and $[Si_4O_{10}]$ for a structure based on the $(4.8^2)_4$ net and having the same unit-cell as that of the $(4.8^2)_4$ net, we carry the structural information on the constituent sheet of tetrahedra in the chemical formula, an obvious advantage.

If we colour the vertices differently in these nets, we may effect the symmetry, size and/or shape of the resulting unit-cells, and hence the stoichiometry in terms of the total numbers of cations and anions, without affecting their ratio. For example, Fig. 8 shows a series of $(6^3)_n$ nets with the different vertex colours red (r) and yellow (y). In Fig. 8*a*, the r-y vertices are arranged in the sequence (ryryry) around all six-membered rings, and the resulting planar unit-cell of the $(6^3)_2$ net is identical to that for the vertex arrangement (r^6) (Fig. 1*b*). In Fig. 8*b*, the r-y vertices are arranged in the sequence (r^2yr^2y)(ry^2ry^2) around alternating six-membered rings, and the resulting unit cell of the planar $(6^3)_8$ net is four times that for the vertex arrangement (r^6) (Fig. 1*b*). In Fig. 8*c*, the r-y vertices are arranged in the sequence (r^3y^3) around all six-membered rings; the resulting unit cell

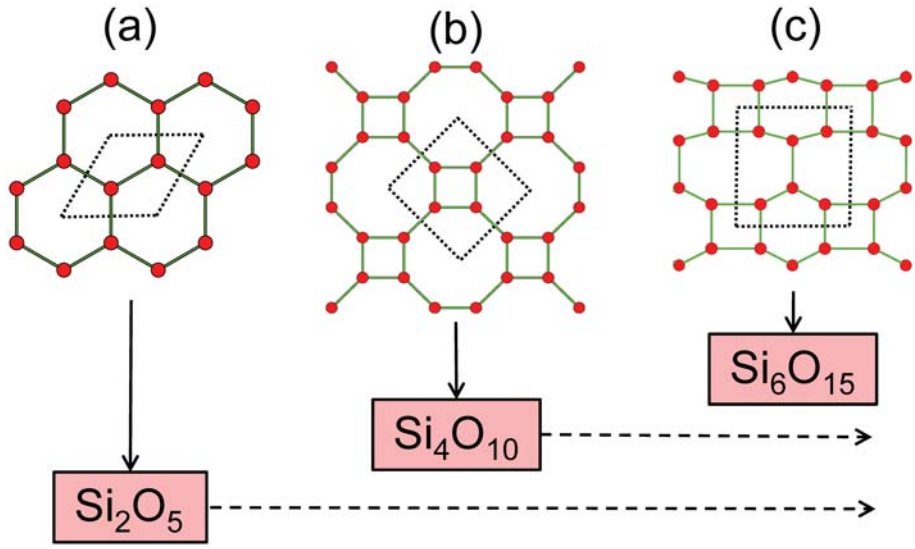

FIG. 7. Some 3-connected plane nets, their unit cells and unit-cell contents; (*a*) the $(6^3)_2$ net; (*b*) the $(4.8^2)_4$ net; (*c*) the $(4.6.8)_4(6.8^2)_2$; legend as in Fig. 1. It is desirable that the corresponding mineral formulae be written in terms of the content of the unit cell of the corresponding net. Thus any formulae with larger numbers of sheet constituents should be represented as multiples (indicated by arrows) of the net unit cell, e.g. $[Si_2O_5]_2$, $[Si_4O_{10}]_3$. Legend as in Fig. 1.

https://doi.org/10.1180/minmag.2015.079.7.17 Published online by Cambridge University Press

of the planar $(6^3)_8$ net is also four times that for the vertex arrangement (r^6) (Fig. 1*b*). In Fig. 8*d*, the r-y vertices are arranged in the sequence $(r^6)(r^3y^3)(y^3r^3)$; the resulting unit cell of the planar $(6^3)_6$ net is not hexagonal and its area is three times that for the vertex arrangement (r^6) (Fig. 1*b*).

Figure 9 shows $(6^3)_n$ sheets of tetrahedra with different patterns of u and d tetrahedra. In Fig. 9*a*, the six-membered rings in **kanemite** ($HNa[Si_2O_8](H_2O)_3$; Garvie *et al*., 1999) have the arrangements (ud^2ud^2) and (u^2du^2d) in a ratio of 1:1 with double the planar unit-cell content of the arrangement (u^6) (Fig. 1). In Fig. 9*b*, the six-membered rings in **gyrolite** ($(Na,Ca_2)Ca_{14}[(Si_{23}Al)O_{60}](OH)_8(H_2O)_{14+x}$; Merlino, 1988) have the arrangements (u^6) and (u_2du_2d) in the ratio of 1:3, and a planar unit-cell four times that of the arrangement (u^6) (Fig. 1). In Fig. 9*c*, the six-membered rings in **palygorskite** ($Mg_5[Si_2O_5]_4(OH)_2(H_2O)_8$; Giustetto and Chiari, 2004) have the arrangements (u^6), (u^3d^3), (d^6) and (d^3u^3) in ratios of 1:1:1:1 and a planar unit-cell four times that of the arrangement (u^6) (Fig. 1). In Fig. 9*d*, the six-membered rings in **kalifersite** ($(K,Na)_5Fe_7^{3+}[Si_{20}O_{50}](OH)_6(H_2O)_{12}$; Ferraris *et al*., 1998) have the arrangements (u^6), (u^3d^3), (d^6) and (d^3u^3) in ratios of 2:1:1:1 and a planar unit-cell four times that of the arrangement (u^6) (Fig. 1). In Fig. 9*e*, the six-membered rings in **sepiolite** ($(Mg,Fe,Al)_4[Si_2O_5]_3(O,OH)_2(H_2O)_4$; Post *et al*., 2007) have the arrangements (u^6), (u^3d^3), (d^6), (d^6) and (d^3u^3) in the ratios 2:1:1:1:1 and a planar unit-cell six times that of the arrangement (u^6) (Fig. 1). In Fig. 9*f*, the six-membered rings in an **antigorite** polysome with m = 16 (e.g. $Mg_{48}[Si_4O_{10}]_{8.5}(OH)_{62}$; Capitani and Mellini, 2006) have the arrangement (u^6),(u^4d^2), (d^6) and (d^2u^4) in the ratios 2:1:3:1 and a planar unit-cell fourteen times that of the arrangement (u^6) (Fig. 1). Obviously there is a large number of different 3-connected sheets with different patterns of u and d tetrahedra, accounting for the numerous modulated sheet-silicate minerals involving tetrahedra at the vertices of $(6^3)_n$ nets.

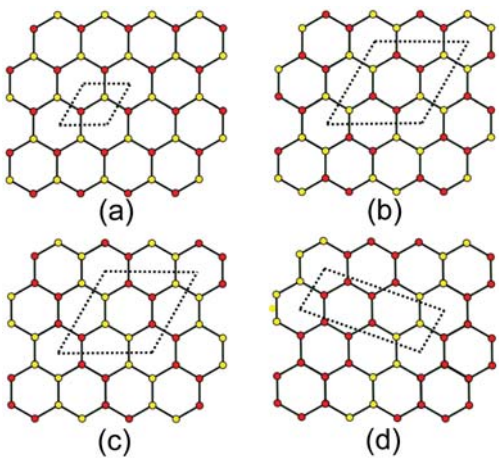

FIG. 8. Different coloured $(6^3)_n$ nets showing the effect of different patterns of red (r) and yellow vertices (y) on the size and shape of the planar unit-cell; (*a*) (ryryry), n = 2; (*b*) (r^2yr^2y), n = 8; (*c*) (r^3y^3), n = 8; (*d*) (r^6) and (r^3y^3), n = 6. Legend as in Fig. 1.

Planar and folded sheets of tetrahedra

In Figs 5*b*,*d*, it is apparent that all the linkages between tetrahedra lie in the same plane, i.e. all O (bridging) anions are exactly in the plane of the net. The same is true of the sheet in Fig. 6. In Fig. 6*b*, the O(bridging) anions are marked by yellow circles, and it is apparent that they lie (approximately) in the plane of the net. This is not the case for all sheets of tetrahedra in silicate minerals. Figure 10*a* shows a sheet with tetrahedra at the vertices of a $(6^3)_n$ net with the tetrahedron arrangements (u^2du^2d) and (ud^2ud^2) in the ratio 1:1. The view in Fig. 10*b* shows that the O(bridging) anions are very non-planar: the sheet is repetitively folded about (fold) axes parallel to the viewing direction.

Figure 11*a* shows a sheet with tetrahedra at the vertices of a $(4.8^2)_n$ net with the tetrahedron arrangements (d^4) and (u^4) in adjacent four-membered rings. The view from both directions (Figs 11*b*,*c*) shows that the O(bridging) anions are very non-planar in each direction, and the sheet in Fig. 11*a* is repetitively folded about (fold) axes parallel to both viewing directions orthogonal to the sheet (Figs 11*b*,*c*). Figure 11*d* shows a sheet with tetrahedra at the vertices of a $(4.6.8)_n$ net. The view in Fig. 11*e* shows that the O(bridging) anions are very non-planar and the sheet is folded parallel to (fold) axes in the viewing direction. In Fig. 11*f*, it can be seen that the O(bridging) anions are very non-planar and yet the sheet is not folded; the folds in the orthogonal direction are seen perpendicular to their fold axis. An oblique view of the sheet in Fig. 11*d* is shown in the ball-and-stick model of Fig. 12; the view directions of Figs 11*e* and 11*f* are shown by arrows in Fig. 12, and the one-directional folding of the sheet is very apparent here.

(u-d) sequences, folding and stoichiometry

The operations of (1) producing u-d sequences in sheets, and (2) folding of sheets do not affect either

https://doi.org/10.1180/minmag.2015.079.7.17 Published online by Cambridge University Press

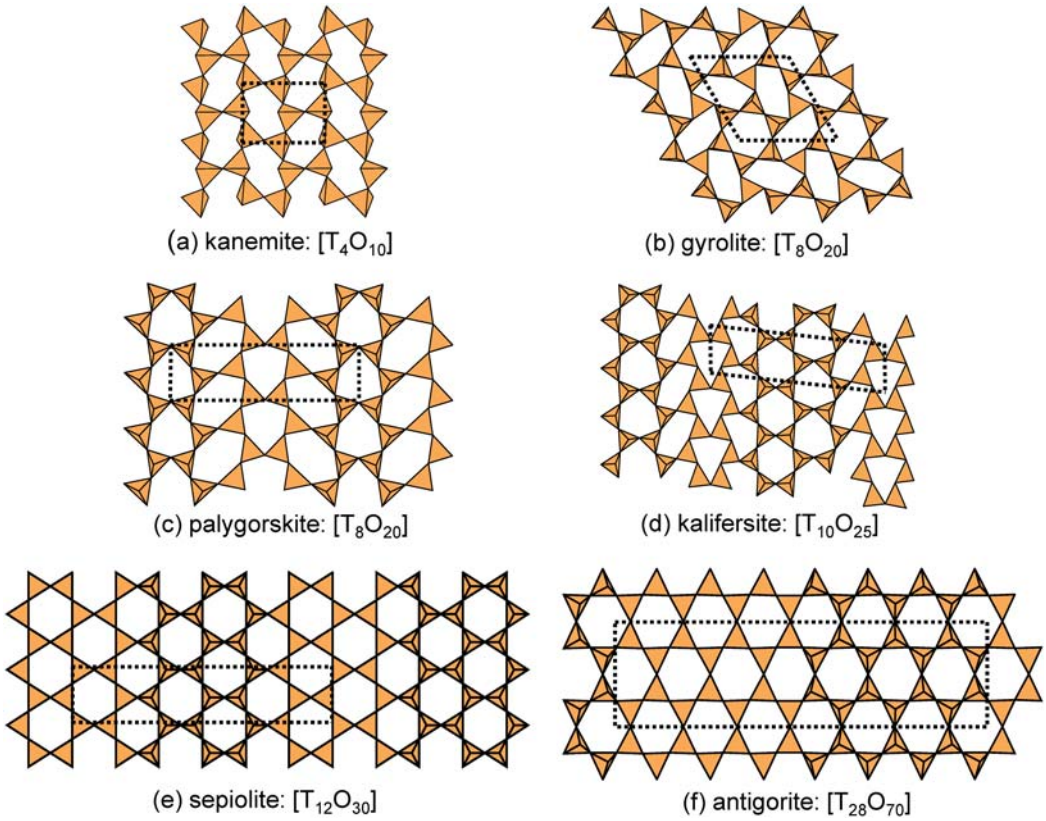

FIG. 9. Different silicate sheets based on planar $(6^3)_n$ nets, showing the effect of different patterns of u and d tetrahedral, the size and shape of the planar unit-cell and the planar unit-cell contents; (*a*) **kanemite**; (*b*) **gyrolite**; (*c*) **palygorskite**; (*d*) **kalifersite**; (*e*) **sepiolite**; (*f*) **antigorite**. Legend as in Fig. 1.

the topology or the stoichiometry of the resultant sheets. This is because these operations are continuous deformations without any breaking of connections, and hence the topology of the sheet is unchanged. Each linkage in a sheet involves an anion shared between two tetrahedra, and hence any changes in linkage of the tetrahedra affects the number of anions in the sheet and changes its stoichiometry.

Oikodoméic operations that change the topology of the parent sheet

I will introduce a series of operations that insert new vertices into a parent net or sheet, thereby changing its topology and stoichiometry. I will designate these as *oikodoméic operations* as they involve the act of building new structural arrangements (from the Greek word oikodomé: the act of building). There are (at least) three classes of oikodoméic operations that may affect nets or connected tetrahedra and include [1] *insertion*, whereby vertices of different connectivity are inserted into the edges of a *parent net*; and [2,3] (local) replication operations whereby a single-layer sheet is replicated, reoriented and linked to the original single-layer sheet to produce a double-layer sheet of tetrahedra.

Insertion of 2-connected vertices into 3-connected plane nets

Although a plane net must contain 3-connected vertices (or a combination of 2- and 4-connected vertices), not all vertices in a topologically plane net need to be 3-connected. In particular, 2-connected vertices may be inserted between 3-connected vertices to produce new plane nets. We will consider insertion of 2-connected vertices into the parent 6^3 net as an example.

https://doi.org/10.1180/minmag.2015.079.7.17 Published online by Cambridge University Press

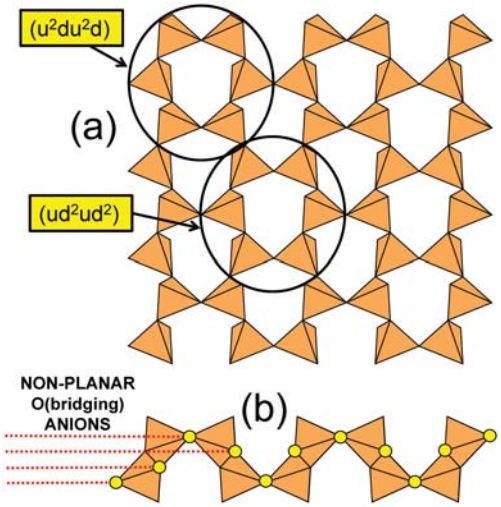

FIG. 10. Folded sheets; (*a*) tetrahedra at the vertices of a $(6^3)_4$ net with apices arranged as (u^2du^2d) and (ud^2ud^2) in adjacent six-membered rings; (*b*), cross-sectional views of the sheet in Fig. 10*a*. Anions involved in T–O–T linkages (bridging anions) are shown as yellow circles, and the dashed red lines mark the various levels of the O(bridging) anions in the horizontal views of the sheets. In Fig. 10*b*, the O(bridging) anions occur at four levels within the sheet and indicate that the sheet is folded (i.e. is non-planar) in this direction.

Consider the labelled graph shown in Fig. 13, in which the vertices are shown as red circles, the edges are shown as green lines, and the edges are labelled 1 to 6. We are interested in the number of different ways in which we may insert 2-connected vertices into a six-membered ring of 3-connected vertices. In terms of Fig. 13, this problem is equivalent to finding the number of distinct ways in which we may colour the edges black or white. To do this, we follow the procedure described by Hawthorne (1983). The symmetric group S_6 is the group whose elements are all permutations of the numbers 1 to 6, and the order of this group is 6! The collection of all permutations of the edge labellings that preserve isomorphism is the automorphism group $\Gamma(G)$ of the graph in Fig. 13. $\Gamma(G)$ is a subgroup of the symmetric group S_6, and the complementary disjoint subgroup of S_6 defines all distinct graphs whose edge sets correspond to the unordered set {1, 2…6}. Let P be a permutation group, a subgroup of S_6, that acts on the set of integers {1, 2…6}. The cycle index of P, $Z(P)$, is the average of the cycle structures of $p \in P$ and may be written as follows:

$$Z(P) = \frac{1}{|P|} \sum_{p \in P} \prod_{k=1}^{N} s_k^{j(k,p)}$$

where s_k are dummy variables and $j(k,p)$ denote

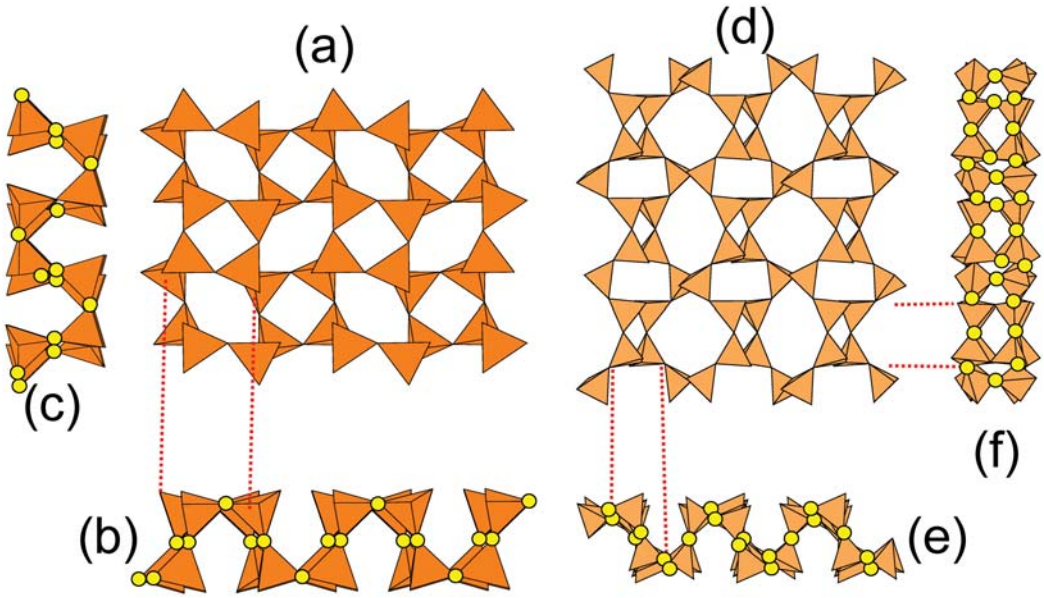

FIG. 11. Folded sheets; (*a*) tetrahedra at the vertices of a $(4.8^2)_n$ net with apices arranged as (d^4) and (u^4) in adjacent 4-membered rings; (*b*), (*c*) cross-sectional views of the sheet in Fig. 11*a*; (*d*) tetrahedra at the vertices of a $(4.6.8)_n$ net; (*e*), (*f*) cross-sectional views of the sheet in Fig. 11*d*. Legend as in Fig. 10.

https://doi.org/10.1180/minmag.2015.079.7.17 Published online by Cambridge University Press

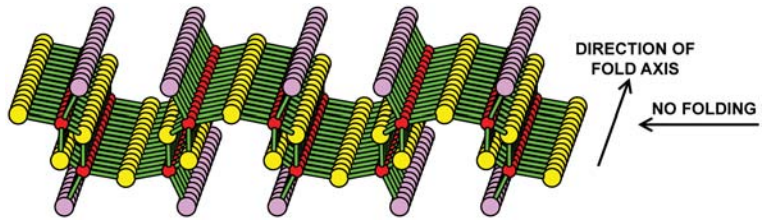

FIG. 12. Folded nets; tetrahedra at the vertices of a $(4.6.8)_n$ net viewed obliquely, with the view directions of Figs 11*e*,*f* shown by arrows. Anions involved in T–O–T linkages (bridging anions) are shown as yellow circles, non-bridging anions are shown as mauve circles, T cations are shown as small red circles. The one-directional folding in Figs 11*d*,*e* is very apparent here.

cycles of length k in the permutation $g \in S$. The symmetry of the graph in Fig. 13 is the plane group *P6m*. The disjoint cycle decomposition and cycle structure of this group are shown in Table2. The cycle index of the group may be derived from the cycle structure given in Table 2 as follows:

$$Z(P) = \frac{1}{12}[s_1^6 + 3s_1^2s_2^2 + 4s_2^3 + 2s_3^2 + 2s_6^1]$$

Let the edges be coloured from the set of two integers (1 = black = no inserted 2-connected vertex; 2 = white = inserted 2-connected vertex). From the unweighted version of Pólya's theorem (Brualdi, 1977; Cohen, 1978), the number of arrangements $|S|$, is given by $Z(P;m)$ where m is the number of colours (2 in this case):

$$\begin{aligned} |S| &= Z(P; m) \\ &= \frac{1}{12}[m^6 + 3m^2m^2 + 4m^3 + 2m^2 + 2m^1] \\ &= 13. \end{aligned}$$

Thus there are 13 distinct arrangements of inserted 2-connected vertices in a six-membered ring of 3-connected vertices. These are illustrated in Fig. 14, and they are labelled by integer strings of 1 and 0 that indicate inserted and non-inserted edges, respectively, reading clockwise from edge 1 (Fig. 14).

The next step is to embed these inserted six-membered rings into $(6^3)_n$ nets. This embedding will generate unit cells of different size, depending on the characteristics of the embedded six-membered ring. When discussing this insertion process, I will refer to the original net as the *parent net*. In the parent $(6^3)_2$ net, the unit cell contains two

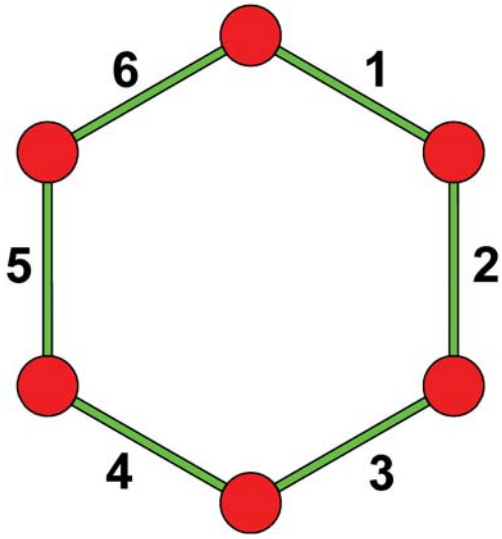

FIG. 13. A six-membered ring of vertices (red circles) connected by labelled edges (green).

TABLE 2. Disjoint cycle decomposition and cycle structure for the automorphism group *P6m*.

Disjoint cycle decomposition	Cycle structure
(1)(2)(3)(4)(5)(6)	s_1^6
(123456)	s_6^1
(135)(246)	s_3^2
(14)(25)(36)	s_2^3
(153)(264)	s_3^2
(165432)	s_6^1
(1)(4)(26)(35)	$s_1^2 s_2^2$
(2)(5)(13)(46)	$s_1^2 s_2^2$
(3)(6)(15)(24)	$s_1^2 s_2^2$
(16)(25)(34)	s_2^3
(12)(36)(45)	s_2^3
(14)(23)(56)	s_2^3

https://doi.org/10.1180/minmag.2015.079.7.17 Published online by Cambridge University Press

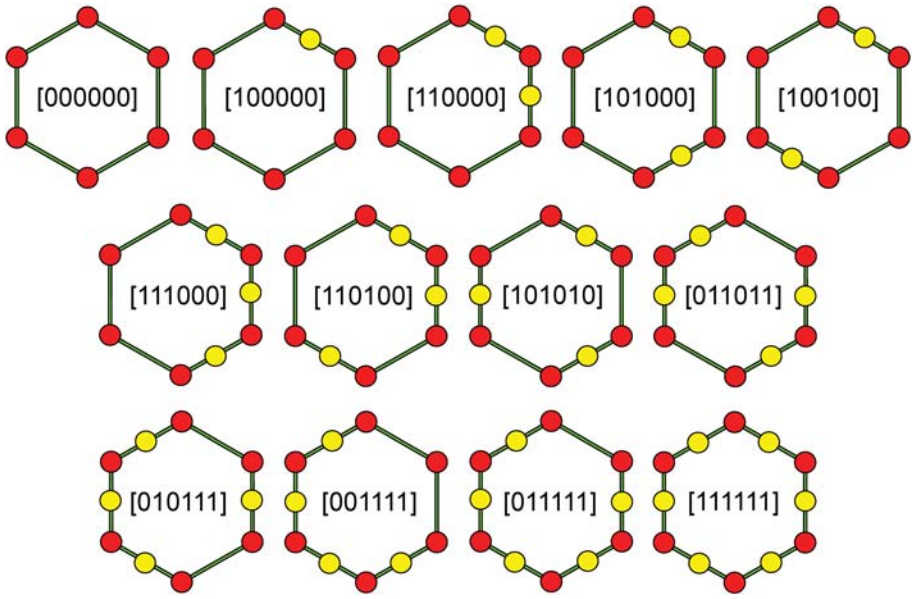

FIG. 14. Distinct arrangements of 2-connected vertices (yellow circles) inserted into the labelled edges of the graph of Fig. 13. Each graph is denoted by an integer string in square brackets, where 0 denotes a non-inserted edge and 1 denotes an inserted edge.

vertices (Fig. 15*a*), and the origin is at the centre of the six-membered ring. If we focus on the translational-symmetry aspects of the net, the position of the origin is not important, and we may consider the elementary building unit as the six-membered ring which then forms the net via the action of translational-symmetry operators in the plane of the net. For the rings in Fig. 14 to be inserted into the parent $(6^3)_2$ net (i.e. with no change in the translational symmetry of the net), the edges of adjacent rings must match. The condition for this to occur is that *trans* edges of the ring constituting the unit cell must be identical, i.e. they must either both contain inserted 2-connected vertices, or both not contain inserted 2-connected vertices. Inspection of Fig. 14 shows that only rings [000000] (the parent net), [100100], [011011] and [111111] satisfy this criterion, i.e. those nets where the net symbols [s_n, $n = 1$–6] satisfy the relation $s_n = s_{n+3}$; the resulting nets are shown in Fig. 15.

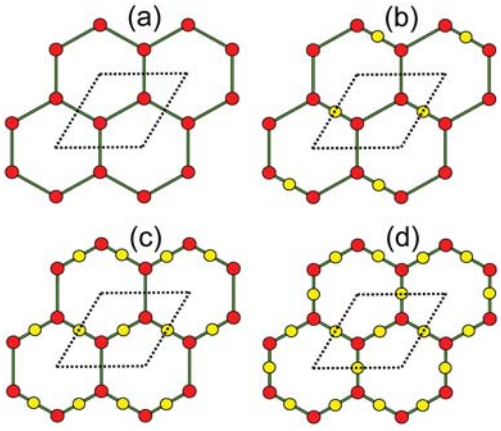

FIG. 15. Plane nets with inserted 2-connected vertices and the same unit-cell size as the parent $(6^3)_2$ net; (*a*) [000000]; (*b*) [100100]; (*c*) [011011]; (*d*) [111111]. Legend as in Figs 1 and 14.

Can the rest of the inserted rings in Fig. 14 be inserted into $(6^3)_n$ nets with larger unit-cells (i.e. $n > 2$)? All except two of them can be inserted into a parent $(6^3)_4$ net with a planar unit-cell of twice the area of the unit cell of the $(6^3)_2$ net. One ring, [111000] (Fig. 14), can be inserted into the parent net with a planar unit-cell of four times the area of the unit cell of the parent net. Finally, one ring, [101010] (Fig. 14), cannot fit into any parent $(6^3)_n$ net; it is left as an exercise for the reader to prove this statement. All the inserted nets with doubled and quadrupled unit-cells relative to that of the $(6^3)_2$ net are illustrated in Figs 16*a–h*.

https://doi.org/10.1180/minmag.2015.079.7.17 Published online by Cambridge University Press

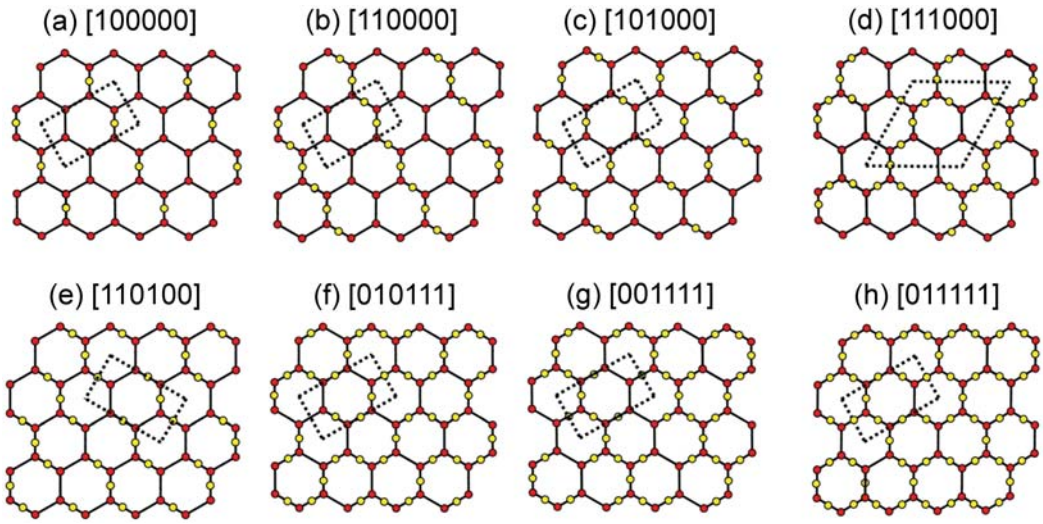

FIG. 16. Plane nets with inserted 2-connected vertices and a unit cell with two- or four-times the area of the unit cell of the parent net; (*a*) [100000]; (*b*) [110000]; (*c*) [101000]; (*d*) [111000]; (*e*) [110100]; (*f*) [010111]; (*g*) [001111]; (*h*) [011111]. Legend as in Figs 1 and 14.

Let us examine Fig. 15 in a little more detail. In Fig. 15*b*, 2-connected vertices have been inserted into one-third of the edges of the parent $(6^3)_2$ net, and the original six-membered rings become eight-membered rings. There are now two types of vertices: 8^2 and 8^3 in the ratio 1:2, and the resulting net is $(8^2)_1(8^3)_2$. In Fig. 15*c*, 2-connected vertices have been inserted into two-thirds of the edges of the parent $(6^3)_2$ net. The original six-membered rings become ten-membered rings, there are two types of vertices: 10^2 and 10^3 in the ratio 1:1, and the resulting net is $(10^2)_2(10^3)_2$. In Fig. 15*d*, 2-connected vertices have been inserted into all edges of the parent $(6^3)_2$ net; the original six-membered rings become twelve-membered rings, there are two types of vertices: 12^2 and 12^3 in the ratio 3:2, and the resulting net is $(12^2)_3(12^3)_2$.

Figure 17 shows the $(8^2)_1(8^3)_2$ net (cf. Fig. 15*b*) and the corresponding net (of tetrahedra) in **esquireite**, $Ba[Si_6O_{13}](H_2O)_7$ (Kampf *et al*., 2015). The net corresponding to the sheet of tetrahedra is fairly planar (Fig. 17*b*), which is to be expected as esquireite is a double-layer sheet silicate, which is sufficient to prevent folding of the sheet.

Figures 18*a*,*b* show the ideal $(10^2)_2(10^3)_2$ net (cf. Fig. 15*c*) and the net of tetrahedra in **tumchaite**, $Na_2(Zr,Sn)Si_4O_{11}(H_2O)_2$ (Subbotin *et al*., 2000). The net corresponding to the sheet of tetrahedra (Fig. 18*b*) is distorted strongly from geometrical planarity (Fig. 18*b*) but is $2 \times (10^2)_2(10^3)_2$ and topologically identical to the ideal inserted net of Fig. 18*a*. This geometrical distortion causes a doubling in the size of the unit cell relative to that of the ideal inserted net (Fig. 18*a*).

Figure 19 shows the ideal $(12^2)_3(12^3)_2$ net (cf. Fig. 15*d*) and the net of tetrahedra in **zephyllite**, $Ca_{13}[Si_5O_{14}]_2F_8(OH)_2\ (H_2O)_6$ (Merlino, 1972, Mikenda *et al*., 1997). The net corresponding to the sheet of tetrahedra is

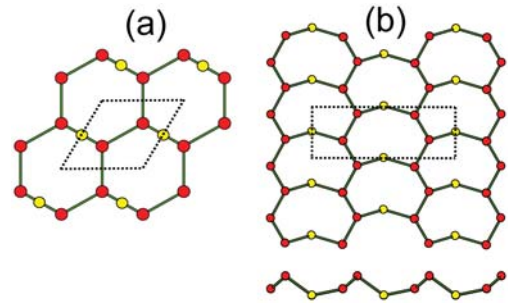

FIG. 17. Nets derived from the 3-connected plane net $(6^3)_2$ by insertion of two 2-connected vertices between 3-connected vertices in a six-membered ring; (*a*) the ideal $(8^2)_1(8^3)_2$ net; (*b*) the $(8^2)_1(8^3)_2$ net of the upper-layer of the double-layer sheet of tetrahedra in the structure of **esquireite** (a double-layer sheet silicate); legend as in Figs 1 and 14.

https://doi.org/10.1180/minmag.2015.079.7.17 Published online by Cambridge University Press

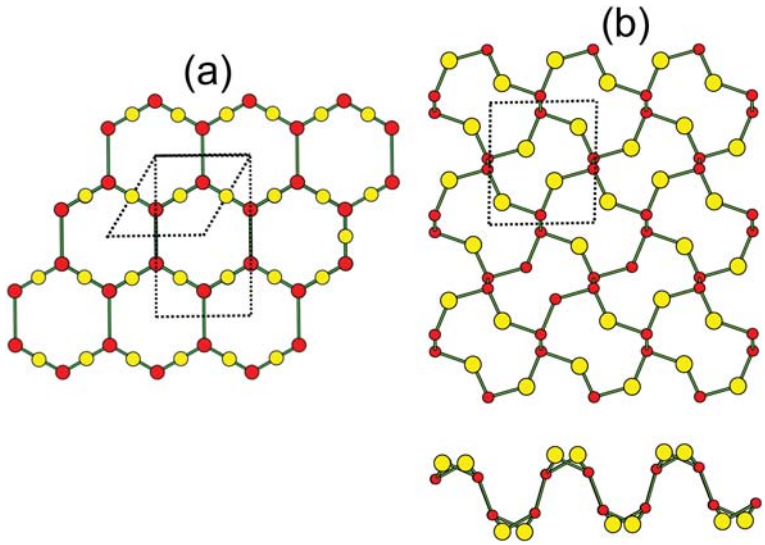

FIG. 18. Nets derived from the 3-connected plane net $(6^3)_2$ by insertion of four 2-connected vertices between 3-connected vertices in a six-membered ring; (*a*) the ideal $(10^2)_2(10^3)_2$ net; (*b*) the $2\times(10^2)_2(10^3)_2$ net in the structure of **tumchaite**; legend as in Figs 1 and 14. Note the very non-planar nature of the net in Fig. 18*b*.

$(12^2)_3(12^3)_2$ (Fig. 19*b*) and is topologically identical to the ideal inserted net in Fig. 19*a*. This net is much less geometrically distorted than the $2\times(10^2)_2(10^3)_2$ net (Fig. 18*b*) and the size of the planar unit-cell in zeophyllite is that of the ideal inserted net. It is tempting to say the much smaller degree of distortion of the $(12^2)_3(12^3)_2$ net of tetrahedra in **zeophyllite** relative to the corresponding net in **tumchaite** is due to the higher symmetry of the net topology in the former.

We may see the effect of insertion on the stoichiometry of the various nets by counting the vertices and edges in the various nets of Fig. 15, omitting Fig. 15*b* for the moment as **esquireite** is a double-sheet silicate and additional factors affect its stoichiometry. Let ^{2}T be a 2-connected vertex and ^{3}T be a 3-connected vertex; (1) the parent net (Fig. 15) is $[^3T_2O_5]$; (2) the net in Fig. 15*c* has the stoichiometry $[^2T_2^3T_2O_{11}]$ which is seen in the formula of **tumchaite**, $Na_2(Zr,Sn)[Si_4O_{11}](H_2O)_2$.

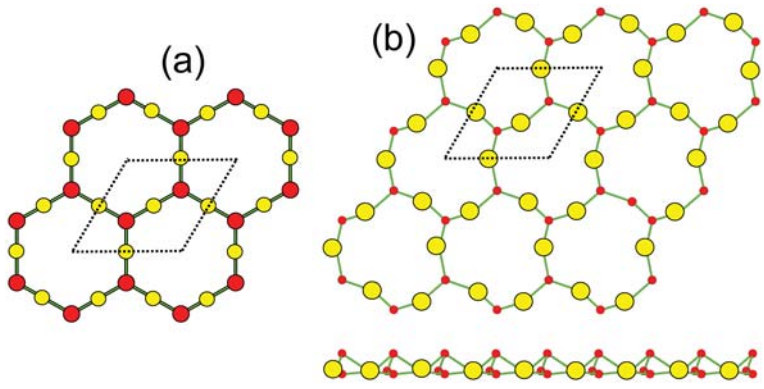

FIG. 19. Nets derived from the 3-connected plane net $(6^3)_2$ by insertion of six 2-connected vertices between 3-connected vertices in a six-membered ring; (*a*) the ideal $(12^2)_3(12^3)_2$ net; (*b*) the $(12^2)_3(12^3)_2$ net in the structure of **zeophyllite**; legend as in Figs 1 and 14. Note the planar nature of the net in Fig. 19*b*.

https://doi.org/10.1180/minmag.2015.079.7.17 Published online by Cambridge University Press

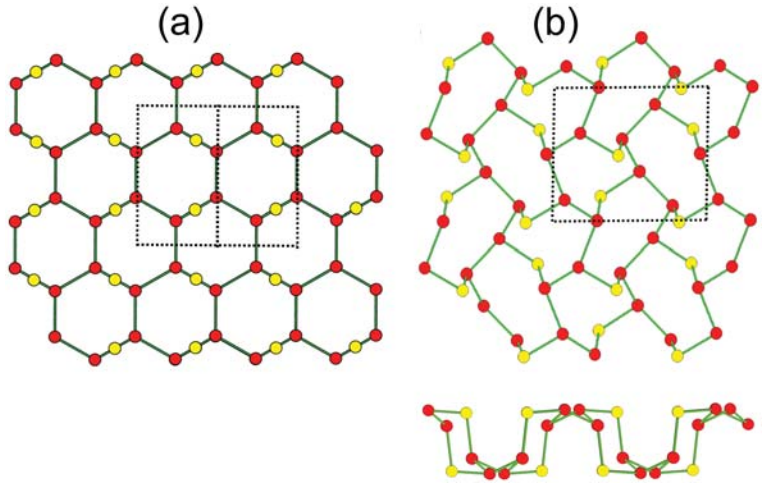

FIG. 20. Nets derived from the 3-connected plane net $(6^3)_4$ by insertion of two 2-connected vertices between 3-connected vertices in a six-membered ring; (*a*) the ideal $(8^2)_4(8^3)_2$ net; (*b*) the $2 \times (8^2)_4(8^3)_2$ net in the structure of **kvanefjeldite**; legend as in Figs 1 and 14. Note the very non-planar nature of the net in Fig. 20*b*.

The net in Fig. 15*d* has the stoichiometry $[^2T_3^3T_2O_{14}]$ which is seen in the formula of **zeophyllite**, $Ca_{13}[Si_5O_{14}]_2F_8(OH)_2(H_2O)_6$; the stoichiometry of the tetrahedron unit in the structure is doubled to avoid a formula with non-integral number of Ca atoms, but we retain the topological unit-cell of the sheet by writing the sheet as $[Si_5O_{14}]_2$ rather than $[Si_{10}O_{28}]$.

It is notable that all inserted nets in Fig. 15 are represented by known structural arrangements. Is this the case for Fig. 16, the nets based on parent nets with unit cells larger than that of the $(6^3)_2$ net? At present, only one of these nets is represented by a mineral structure: [101000] in Fig. 16*c*. Figure 20 shows the $(8^2)_2(8^3)_4$ net of tetrahedra in **kvanefjeldite**, $Na_4(Ca,Mn)[Si_6O_{16}]$ (Johnsen *et al*., 1983). The net corresponding to the sheet of tetrahedra is strongly geometrically distorted (Fig. 20*b*), but is $2 \times (8^2)_2(8^3)_4$ and topologically identical to the ideal inserted net in Fig. 20*a*. This geometrical distortion causes a doubling in the size of the unit cell relative to that of the ideal inserted net (Fig. 20*a*). At present, there are no minerals corresponding to the other nets in Fig. 16. It seems significant that all possible inserted nets with unit cells of the same size as the parent net occur as mineral structures, whereas only one of the inserted nets with unit cells larger than that of the parent net occur as a mineral structure.

It is apparent from the above discussion that the mechanism of *insertion* is a significant building operation in Nature's design of sheet silicates. This insertion mechanism may, in principle, be used on the other 3-connected plane nets described above to produce nets analogous to those derived from the 6^3 plane net. However, at the moment, all known examples of insertion of 2-connected tetrahedra into single-layer 3-connected sheets occur only for sheets based on the 6^3 net (*sensu lato*).

4-connected vertices in plane nets

Several single-sheet silicate minerals contain 4-connected tetrahedra. Insertion of 4-connected vertices into 3-connected plane nets requires changing a pre-existing 3-connected vertex into a 4-connected vertex, and although this is simple enough from a graphical perspective, a crystal structure has very strict geometrical requirements that are not easy to incorporate into such a process. Another way to accomplish this is by inserting pairs of 2-connected vertices into the edge of a 3-connected net where the 2-connected vertices do not share a common edge (i.e. they are not connected to each other). The way in which this may be done is shown in Fig. 21. Consider the fragment of the 6^3 net in Fig. 21*a*; a pair of 2-connected vertices is inserted at X, and an oblique view of this arrangement (Fig. 21*b*) shows that (1) the 2-connected vertices do not link to each other, and (2) the initial 3-connected vertices are

https://doi.org/10.1180/minmag.2015.079.7.17 Published online by Cambridge University Press

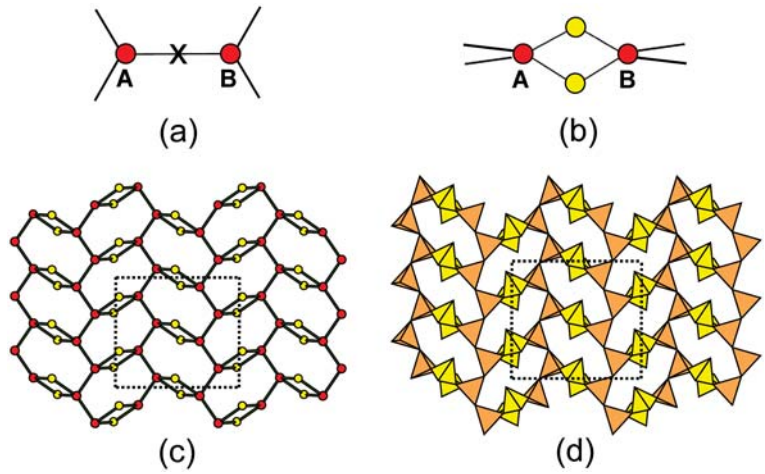

FIG. 21. Insertion of pairs of 2-connected vertices into an edge of the 6^3 net; (*a*) an edge of the 6^3 net and the position, X, at which the pair of 2-connected vertices is inserted; (*b*) oblique view of (*a*), showing the pair of 2-connected vertices and how the 3-connected vertices of the parent net become 4-connected; (*c*) the net in **amstallite**; (d) the sheet of tetrahedra in **amstallite**. Yellow vertices and tetrahedra are 2-connected.

transformed into 4-connected vertices. This mechanism, operating on one set of *trans* edges in the 6^3 net produces the net in Fig. 21*c*. The corresponding sheet of 2- and 4-connected tetrahedra (Fig. 21*d*) occurs in the structure of amstallite ($CaAl(OH)_2[AlSi_3O_8(OH)_2](H_2O$; Quint, 1987).

Single-layer sheet-silicate minerals containing 4-connected tetrahedra generally do not contain 2-connected tetrahedra, and different oikodoméic operations must be operative. For example, [1] the **melilite-group minerals** (e.g. **meliphanite**, $(Na,Ca)_4Ca_4[Be_4AlSi_7O_{24}(F,O)_4]$; Grice and Hawthorne (2002) and **vladykinite**, $Na_3Sr_4[(Fe^{2+}Fe^{3+})Si_8O_{24})$; Chakhmouradian *et al*., 2014) contain clusters of 3-connected tetrahedra linked into sheets by 4-connected tetrahedra; [2] **semenovite**, $(Ca,Na)_8Na_{0-2}REE_2(Fe,Ti)[(Si,Be)_{10}(O,F)_{24}]_2$; (Mazzi *et al*., 1979), **busseyite-(Ce)**, $(Ce,Ca)_3(Na,H_2O)_6Mn[Si_9Be_5(O,OH)_{30}(F,OH)_4]$ (Grice *et al*., 2009), and **ferronordite**, $Na_3SrFeSi_6O_{17}$ (Bakakin *et al*., 1970), consist of chains of 3-connected tetrahedra linked into sheets by 4-connected tetrahedra; [3] **prehnite**, $Ca_2Al[Si_3AlO_{10}](OH)_2$ (Papike and Zoltai, 1967), contains only 2-connected and 4-connected tetrahedra in its sheet. Thus at the moment, there seems to be no simple way of generating single-layer sheets of tetrahedra containing 4-connected tetrahedra by insertion of 4-connected tetrahedra into single-layer sheets of 3-connected tetrahedra.

An alternative approach to this issue is to insert 2- and 3-connected vertices into 4-connected nets. Consider the $(4^4)_1$ net shown in Fig. 22*a*. We may insert 2-connected vertices along some of the edges in the $(4^4)_1$ net to produce, for example, the $(4^2)_1(4^4)_1$ net of Fig. 22*b*, and we may insert 3-connected vertices in the same way to produce, for example, the $(4^3)_2(4^4)_2$ net of Fig. 22*c*. If one introduces two *cis* 3-connected vertices into a single four-membered ring, the requirements of matching imposed by the translational symmetry produces a completely inserted net; to obtain a half-inserted net, only half the four-membered rings can be inserted, with the result that the unit cell is doubled relative to that of the parent net.

Figure 23*a* shows the structure of **prehnite** in which chains of 4-connected tetrahedra are cross-linked into a sheet by single 2-connected tetrahedra. The corresponding net is shown in Fig. 23*b*. It consists of a parent $(4^4)_1$ net with two 2-connected vertices inserted into two *cis* edges of each four-membered ring of 4-connected vertices, producing a $(6^2)_2(6^4)_2$ net. Figure 23*c* shows the analogous geometrically idealized net in which it is obvious that the transitivity requirements of translational symmetry require edge-adjacent squares to be oriented differently (i.e. rotated by 180° about an axis orthogonal to the net).

Figure 24*a* shows the structure of **meliphanite**, a structure related to that of the minerals of the

https://doi.org/10.1180/minmag.2015.079.7.17 Published online by Cambridge University Press

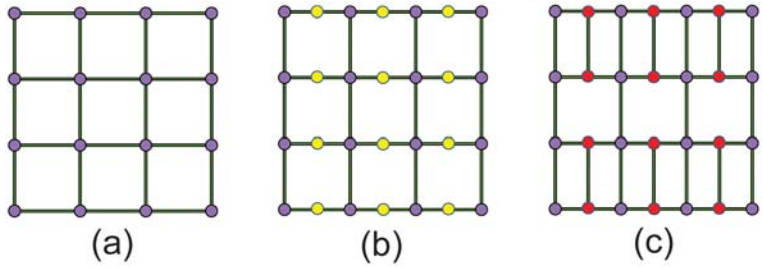

FIG. 22. Insertion of 2- and 3-connected vertices into a $(4^4)_1$ net; (*a*) the $(4^4)_1$ net; (*b*) insertion of 2-connected vertices into the $(4^4)_1$ net; (*c*) insertion of 3-connected vertices into the $(4^4)_1$ net. Legend as in Figs 1 and 14, plus 4-connected vertices are shown as mauve circles.

mellilite group, in which isolated 4-connected tetrahedra are linked by dimers of 3-connected tetrahedra. The corresponding net is shown in Fig. 24*b*. It consists of a parent $(4^4)_1$ net completely inserted with 3-connected vertices, producing a $(5^3)_8(5^4)_4$ net; the analogous geometrically idealized net is shown in Fig. 24*c*. The 3-connected vertices occupying *trans* edges of the original $(4^4)_1$ net link across the original four-membered ring, and the transitivity requirements of translational symmetry require edge-adjacent squares to be oriented differently (i.e. rotated by 90° about an axis orthogonal to the net).

We will see later that 4-connected tetrahedra also occur in double-layer sheet silicates, but they are introduced into the structure by a different process.

Double-layer sheets

The formation of a double-layer sheet via condensation of two single-layer sheets through a plane parallel to the single-layer sheet is illustrated in Fig. 25. Tetrahedra lie at the vertices of a $(6^3)_2$ net, and in Fig. 25*a*, all visible tetrahedra in the six-membered rings have their tetrahedra in the (d^6) arrangement. However, viewing perpendicular to the sheet (Figs 25*b*,*c*) shows that there is another layer of tetrahedra directly underlying the upper layer, and that the tetrahedra of the lower six-membered rings have their vertices in the (u^6) arrangement. The result is that all tetrahedra become 4-connected, the sheet of Fig. 25 has horizontal mirror (or pseudo-mirror) symmetry and is a double-layer sheet.

Oikodoméic operations that produce double-layer sheets

Above, we introduced class-1 oikodoméic operations to construct new nets; thus the operation of *insertion* introduced (for example) 2-connected vertices into 3-connected nets to increase the sizes of the rings of vertices and change the vertex connectivity. Here, we will consider replication

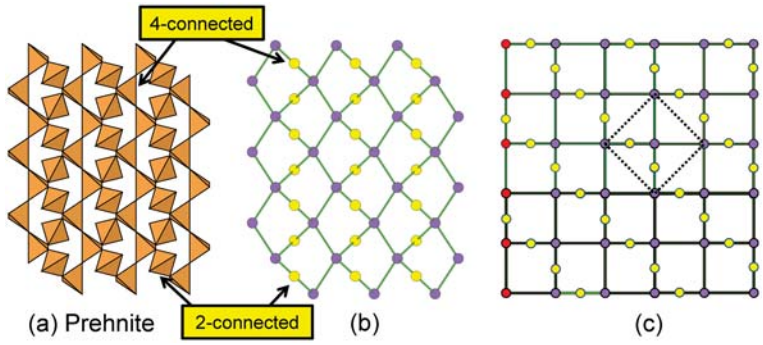

FIG. 23. Tetrahedra in **prehnite**; (*a*) the sheet of 2- and 4-connected tetrahedra; (*b*) the net corresponding to the sheet in Fig. 23*a*; (*c*) geometrically adjusted net of Fig. 23*b*. Legend as in Fig. 22.

https://doi.org/10.1180/minmag.2015.079.7.17 Published online by Cambridge University Press

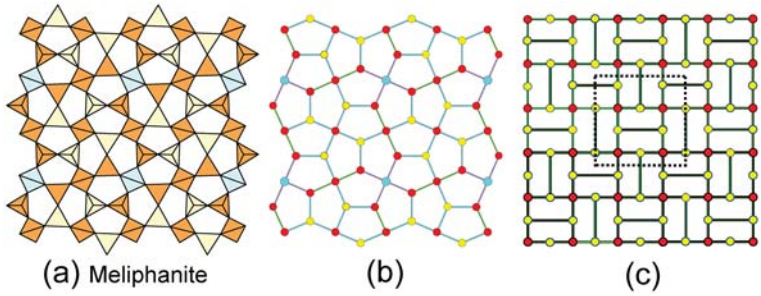

FIG. 24. Tetrahedra in meliphanite; (*a*) the sheet of 3- and 4-connected tetrahedra; (*b*) the net corresponding to the sheet in Fig. 24*a*; (c) geometrically adjusted net of Fig. 24*b*. Orange: 3-connected (SiO_4) tetrahedra; blue: 4-connected (AlO_4) tetrahedra; yellow: 3-connected (BeO_4) tetrahedra.

operations whereby a parent single-layer sheet is replicated in a different orientation and linked to the original single-layer sheet to produce a double-layer sheet of tetrahedra: class-2 and class-3 oikodoméic operations. There is an additional advantage of considering double-layer sheet arrangements of tetrahedra in this fashion. In Fig. 25, the symbols of double-layer nets are much more complicated and more difficult to derive that those of single-layer nets, and this problem becomes much more acute in the more complicated plane nets with both u and d configurations in their corresponding rings of tetrahedra. We may circumvent this problem by using the symbol of the plane net and adding the oikodoméic operations that generate the final net or tetrahedron arrangement: thus, for example, we represent the sheet in Fig. 25 as 6^3 $(u^6)+m$, where it is understood that the oikodoméic mirror operator acts through the specified apical vertices. How do these oikodoméic operations differ from symmetry operators? A symmetry element is part of the symmetry of an already existing arrangement, and the corresponding symmetry operation describes the transformation of part of the arrangement to geometrical congruence with another part of the arrangement, whereas oikodoméic operations generate arrangements with the corresponding (topological) symmetry from a simpler parent arrangement of tetrahedra. Thus the $(6^3)_2$ single-layer sheet of tetrahedra in Fig. 25*a* will generate the double-layer sheet of tetrahedra in Figs 25*b*,*c* *via* an oikodoméic mirror operation through the plane of the apical anions of the parent sheet in Fig. 25. I emphasize that the atomic arrangement generated by an oikodoméic operation is topologically (but not necessarily geometrically) congruent with the original single-layer sheet of tetrahedra.

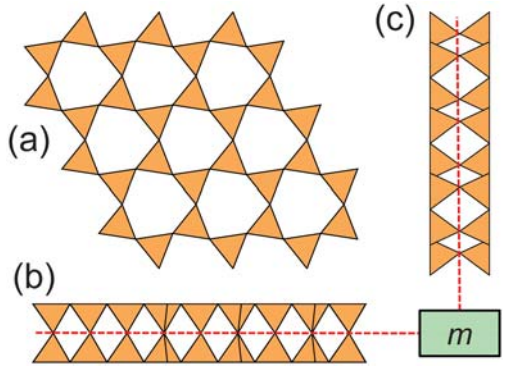

FIG. 25. (*a*) a $(6^3)_2$ net of 3-connected tetrahedra with all visible six-membered rings in the (d^6) arrangement; (*b*), (*c*) horizontal views of Fig. 25*a*, showing that it consists of two layers of tetrahedra that point in the d and u directions such that all tetrahedra in the upper single-layer sheet link to tetrahedra in the lower single-layer sheet, imparting horizontal (possibly pseudo-) mirror symmetry to the overall double-layer sheet.

Figure 26 illustrates four possible oikodoméic operators of this sort, showing how tetrahedra of a single-layer sheet may be replicated and linked to those of the parent single-layer sheet to form a double-layer sheet. In Figs 26*a* and 26*b*, the tetrahedra of the parent sheet are replicated by a horizontal mirror operation and a horizontal two-fold rotation operation, respectively; I refer to these as class-2 oikodoméic operators which I define as passing through an apical anion of a d tetrahedron. In Figs 25*c* and 25*d*, some tetrahedra of the original sheet are reoriented by a horizontal mirror operation and a horizontal two-fold rotation operation, and the remaining tetrahedra are replicated by a horizontal mirror operation and a horizontal two-

https://doi.org/10.1180/minmag.2015.079.7.17 Published online by Cambridge University Press

fold rotation operation, respectively; I refer to these as class-3 oikodoméic operators which I define as passing through the central cation of a d tetrahedron. The operation shown in Fig. 26*a* is widely known in the science of framework silicates (particularly zeolites) as a *sigma operation*, and is used for framework structures to build more complicated nets (frameworks of tetrahedra) from more simple arrangements.

The mirror operator illustrated in Fig. 26*a* is the most common oikodoméic operator in sheet silicates. Figure 27 shows the parent single-layer sheet and the double-layer sheet of tetrahedra in the structure of **macdonaldite**, $BaCa_4[Si_{16}O_{36}(OH)_2](H_2O)_{10}$ (Cannillo *et al*., 1968). The parent single-layer sheet is based on the $(4.8^2)_4$ net, and an oikodoméic mirror operation through all apical anions of the d tetrahedra produces the double-layer sheet of macdonaldite. Figure 28 shows the parent single-layer sheet and the double-layer sheet of tetrahedra in the structure of **naujakasite**, $Na_6(Fe^{2+},Mn^{2+})Al_4Si_8O_{26}$ (Basso *et al*., 1975). The parent single-layer sheet is based on the $(6^3)_{12}$ net with an oikodoméic two-fold rotation operator through all apical anions of the d tetrahedra. Figure 29 shows the parent single-layer sheet and the double-layer sheet of tetrahedra in the structure of **zussmanite**, $K(Fe,Mg,Mn)_{13}[(Si,Al)_{18}O_{42}](OH)_{14}$ (Lopes-Vieira and Zussman, 1969). It is based on the $(3.8^2)_6(6.8^2)_6$ net with an oikodoméic mirror operator through the central T cation of the d tetrahedra. Figure 30 shows the parent single-layer sheet and the double-layer sheet of tetrahedra in the structure of **lemoynite**, $(Na,K)_2CaZr_2Si_{10}O_{26}.(H_2O)_{5–6}$ (Blinov *et al*., 1975; LePage and Perrault, 1976). Figures 30*a* and 30*b* show the net and upper sheet in **lemoynite**, a parent $(6^3)_2$ net with each six-membered ring having four pairs of 2-connected vertices (one u and one d) inserted in four of the six edges of each six-membered ring to form a $(14^2)_8(14^3)_4$ net based on fourteen-membered rings, and an oikodoméic two-fold rotation axis through the centres of the 2-connected tetrahedra pointing down (the blue tetrahedra in Fig. 30). Figure 30*c* shows the lower sheet in **lemoynite**, again a $(14^2)_8(14^3)_4$ net, but rotated 180° in the horizontal plane such that the original 2-connected tetrahedra are now 4-connected, as shown in Fig. 30*d*. The black circles in Figs 30*b*,*c*,*d* focus on how the oikodoméic two-fold rotation

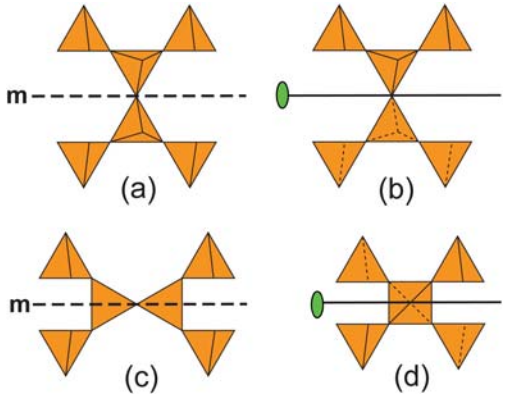

FIG. 26. Oikodoméic operations replicating and reorienting the upper single-layer tetrahedra from above the plane of the operation to below the plane of the operation; (*a*) the mirror operation acting though apical anions of the upper single-layer parent sheet; (*b*) the two-fold rotation operation acting though apical anions of the upper single-layer parent sheet; (*c*) the mirror operation though the central T cations of tetrahedra shared between the upper and lower single-layer sheets; (*d*) the two-fold rotation operation acting though the central T cations of tetrahedra shared between the upper and lower single-layer sheets.

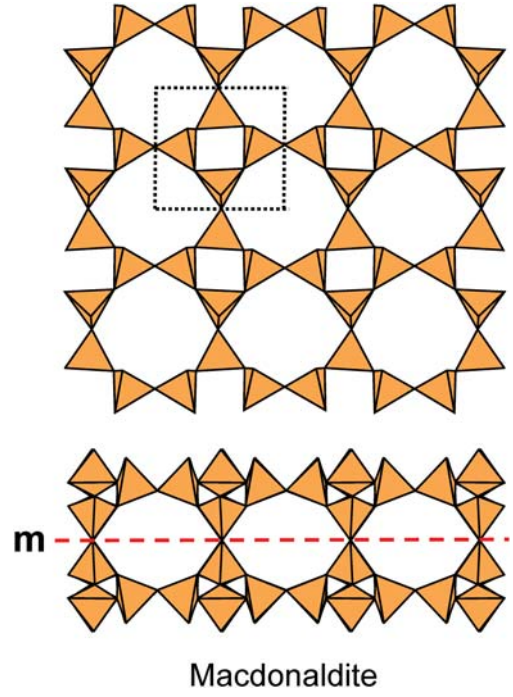

FIG. 27. The upper single-layer sheet in **macdonaldite** (above), which is based on the $(4.8^2)_4$ net and has the u-d configuration $(u^3d^1)(u^2du^4d^1)$, and the complete double-layer sheet viewed edge-on. The position of the oikodoméic mirror operator is indicated by the broken red line and the letter **m**.

https://doi.org/10.1180/minmag.2015.079.7.17 Published online by Cambridge University Press

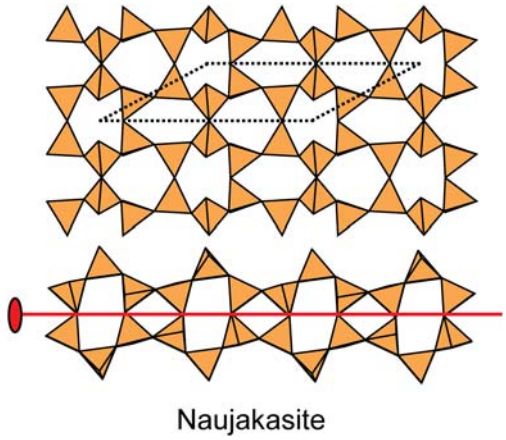

FIG. 28. The upper single-layer sheet in **naujakasite** (above), which is based on the $(6^3)_4$ net and has the u-d configuration $(u^2d^4)(ud^2ud^2)$, and the complete double-layer sheet (below) viewed edge-on. The position of the oikodoméic two-fold rotation operator is indicated by the red line and the symbol for a two-fold rotation.

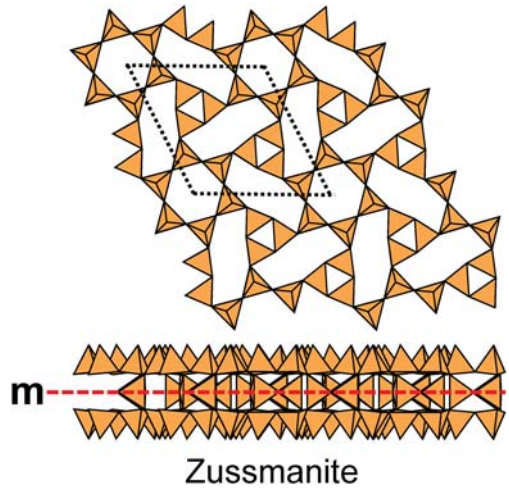

FIG. 29. The upper single-layer sheet in **zussmanite** (above), which is based on the $(3.8^2)_6(3.8^2)_6$ net and has the u-d configuration $(u^3d^1)(u^2du^4d^1)$, and the complete double-layer sheet (below) viewed edge-on. The position of the oikodoméic mirror operator is indicated by the broken red line and the letter **m**.

operator produces a 4-connected tetrahedron (blue in Fig. 30) in the double-layer sheet. The cross-section of the sheet in Fig. 30*e* shows the oikodoméic two-fold operation through the central T cations of the initially 2-connected d tetrahedra of the upper sheet (Fig. 30*b*).

The effect of oikodoméic operations on tetrahedron connectivity

Figure 31 shows an oikodoméic mirror operation on a single-layer 3-connected sheet with both u and d tetrahedra. In the parent sheet, all tetrahedra are 3-connected. In the double-layer sheet, all u tetrahedra are 3-connected as the upward apical anions (shown as red circles in Fig. 31) do not link to any other tetrahedra (i.e. the apical anions are 1-connected). However, all d tetrahedra are 4-connected as the downward apical anions (shown as green circles in Fig. 31) link to tetrahedra in the lower single-layer sheet (i.e. the apical anions are 2-connected). An oikodoméic two-fold rotation operation through the downward apical anions (as in **naujakasite**, Fig. 28) has the same effect on connectivity as the oikodoméic mirror operation through downward apical anions. An oikodoméic mirror operation through the central T cation of the d tetrahedra (as in **zussmanite**, Fig. 29) and an oikodoméic two-fold rotation operation through the central T cation of the d tetrahedra (as in lemoynite, Fig. 30) change the 3-connected d tetrahedra of a parent single-layer sheet into 4-connected tetrahedra of a double-layer sheet.

Incomplete oikodoméic operations

We must also recognize the possibility that an oikodoméic operator may replicate only part of the upper single-layer sheet in the lower single-layer sheet, and that this type of incomplete operation also affects the stoichiometry of the resultant double-layer sheet (see below). Figure 32 shows a hypothetical example in which alternate tetrahedra in the upper single-layer sheet are not replicated in the lower single-layer sheet, and the bond-valence requirements of the non-bridging apical anions are satisfied by hydrogen atoms, forming acid silicate groups. Obviously, the effect of incomplete replication of the upper single-layer sheet must be incorporated into any relation between connectivity and stoichiometry.

The effect of tetrahedron connectivity on stoichiometry

Insertion of 2-connected vertices into 3-connected nets

Consider the 3-connected tetrahedron shown in Fig. 33*a*. Three anions are linked to two Si atoms

https://doi.org/10.1180/minmag.2015.079.7.17 Published online by Cambridge University Press

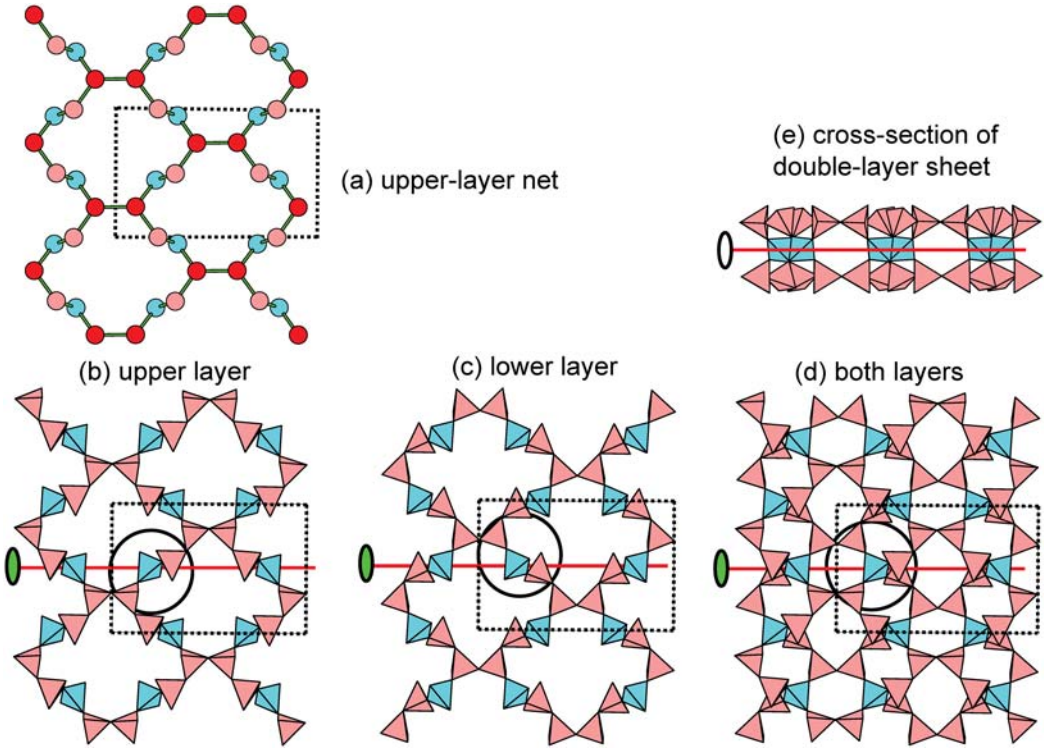

FIG. 30. The silicate unit in the structure of **lemoynite**; (*a*) the upper-layer net consisting of a $(6^3)_2$ parent net (vertices shown in red) with pairs of 2-connected vertices (in blue and pink) inserted along four of the six edges of the parent net, resulting in a $(14^3)_{12}$ net; (*b*) the upper layer of 2- and 3-connected tetrahedra (pink) and the central 2-connected tetrahedra (green); (*c*) the lower layer of 2- and 3-connected tetrahedra (pink) and the central 2-connected tetrahedra (green); (*d*) the complete double-layer sheet in plan; and (e) the complete double-layer sheet in cross-section. The position of the oikodoméic two-fold rotation operator is indicated by the red line and the symbol for a two-fold rotation.

and hence contribute one-half an anion each to the overall stoichiometry of the tetrahedron, and one anion is linked to one Si atom and hence contributes one anion to the overall stoichiometry. The result is a tetrahedron stoichiometry that consists of one Si and $3 \times 0.5 + 1 \times 1 = 2.5$ anions: $SiO_{2.5}$.

Consider the 2-connected tetrahedron shown in Fig. 33*b*. Two anions are linked to two Si atoms and hence contribute one-half an anion each to the overall stoichiometry of the tetrahedron, and two anions are each linked to one Si atom and hence contribute one anion each to the overall stoichiometry. The result is a tetrahedron stoichiometry that consists of one Si and $2 \times 0.5 + 2 \times 1 = 3.0$ anions: SiO_3.

Consider the structures of **tumchaite**, $Na_2(Zr, Sn)Si_4O_{11}(H_2O)_2$ (Subbotin *et al.*, 2000), and

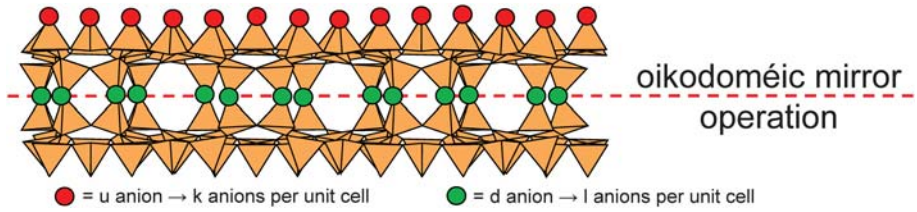

FIG. 31. An oikodoméic mirror operation on a parent 3-connected single-layer sheet to produce a double-layer sheet. The operation causes all d tetrahedra of the parent upper single-layer sheet to become 4-connected.

https://doi.org/10.1180/minmag.2015.079.7.17 Published online by Cambridge University Press

zeophyllite (Merlino, 1972; Mikenda *et al*., 1997), both of which are single-layer sheet-silicate minerals based on the $(6^3)_2$ net with inserted 2-connected vertices (Figs 18 and 19). The net in tumchaite is $(10^2)_1(10^3)_1$ (Fig. 18*a*) and the unit cell of the net contains two 2-connected vertices and two 3-connected vertices. Inspection of Figs 33*a*,*b* shows that the resulting stoichiometry of the unit cell of the corresponding sheet will be $TO_3 \times 2 + TO_{2.5} \times 2 = [T_4O_{11}]$, which accords with the formula of **tumchaite**: $Na_2(Zr,Sn)[Si_4O_{11}](H_2O)_2$. The net in **zeophyllite** is $(12^2)_3(12^3)_2$ (Fig. 19*a*) and the unit cell of the net contains three 2-connected vertices and two 3-connected vertices. Inspection of Figs 33*a*,*b* shows that the resulting stoichiometry of the unit cell of the corresponding sheet will be $TO_3 \times 3 + TO_{2.5} \times 2 = [T_5O_{14}]$, which accords with the formula of **zeophyllite**: $Ca_{13}[Si_5O_{14}]_2F_8(OH)_2\ (H_2O)_6$. Note that the unit cell of **zeophyllite** itself is doubled relative to that of the silicate net because of the odd number of Ca atoms in the (doubled) formula.

Insertion of 2- and 3-connected vertices in 4-connected nets

Consider the 4-connected tetrahedron shown in Fig. 33*c*. All four anions are linked to two Si atoms and hence contribute one-half an anion each to the overall stoichiometry of the tetrahedron. The result is a tetrahedron stoichiometry that consists of one Si and $4 \times 0.5 = 2.0$ anions: SiO_2.

Consider the structures of **prehnite** and **meliphanite** (Dal Negro *et al*., 1967; Grice and Hawthorne, 2002), both of which are single-layer sheet-silicate minerals based on the 4^4 net with inserted 2- and 3-connected vertices, respectively (Figs 23 and 24). The net in prehnite is $(6^2)_2(6^4)_2$ (Figs 23*b*,*c*) and the unit cell of the net contains four 2-connected vertices and four 4-connected vertices. Inspection of Figs 33*a*,*c* shows that the resulting stoichiometry of the unit cell of the corresponding sheet will be $TO_3 \times 2 + TO_2 \times 2 = [T_4O_{10}]$, which accords with the formula of **prehnite**: $Ca_2Al[AlSi_3O_{10}](OH)_2$. The net in **meliphanite** is $(5^3)_8(5^4)_4$ (Figs 24*b*,*c*) and the unit cell of the corresponding sheet contains eight 3-connected vertices and four 4-connected vertices. Inspection of Figs 33*b*,*c* shows that the resulting stoichiometry of the unit cell of the net will be $TO_{2.5} \times 8 + TO_2 \times 4 = [T_{12}O_{28}]$, which accords with the formula of **meliphanite**: $Ca_4(Na_3Ca)[Be_4AlSi_7O_{24}F_4]\ (H_2O)_6$.

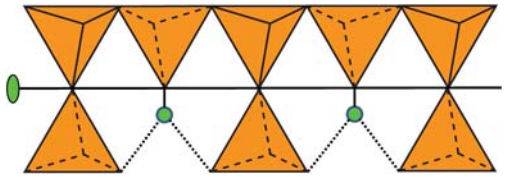

FIG. 32. A hypothetical incomplete oikodoméic two-fold-rotation operation whereby alternate tetrahedra in the upper single-layer parent sheet are not replicated in the lower single-layer sheet, and the 1-connected apical anions thus produced are linked to hydrogen atoms to form acid silicate groups. Green circles: H atoms; dotted lines: hydrogen bonds.

Formula-generating functions and structure-generating functions

Above, we have briefly considered the relation between chemical formula and structural

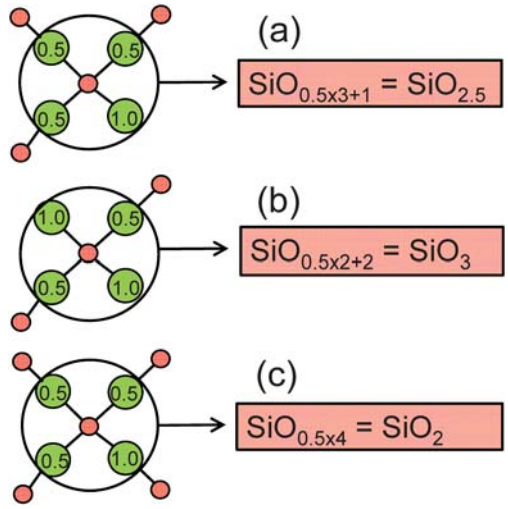

FIG. 33. The relation between tetrahedron connectivity and stoichiometry; (*a*) a 3-connected tetrahedron (i.e. three 2-connected and one 1-connected anions); (*b*) a 2-connected tetrahedron (i.e. two 2-connected anions and two 1-connected anions); (*c*) a 4-connected tetrahedron (i.e. four 2-connected anions). Red circles: T cations; green circles: O anions; in counting the contribution of the tetrahedron to the stoichiometry, each anion shared between two T cations counts as one-half (0.5 in the figure) and each apical anion counts as one (1.0 in the figure). The simplest stoichiometries are thus $SiO_{2.5}$, SiO_3 and SiO_2, respectively.

https://doi.org/10.1180/minmag.2015.079.7.17 Published online by Cambridge University Press

arrangement: one generally cannot 'calculate' the structural arrangement from the chemical formula. Hawthorne (2012) investigated this issue with the T–O–T biopyriboles and structurally related H–O–H Ti-silicates, and proposed that we write very general formulae for related series of minerals such that we may generate known minerals of this type and potential minerals of related structure by incorporating information on local bond-topology into their chemical formulae. Here, I will develop an analogous idea for the sheet-silicate part of sheet-silicate minerals, using this approach as a basis. In this regard, a 'formula-generating function' is an expression that generates the chemical formula (of the sheet-silicate component of a structure) from aspects of a structure with specific bond-topological characteristics: $F_{(i,j\ldots)} = f(i,j\ldots)$, where i, j … are integers describing some topological aspects of the structure. A 'structure-generating function' is an expression that generates the translationally symmetric structural arrangement (of the sheet-silicate component of a structure) from aspects of a structure with specific bond-topological characteristics, and consists of the analogous formula-generating function together with a translationally symmetric net with which the bond-topological characteristics of the formula-generating function may be associated. Thus the function $F_{(i,j\ldots)} = f(i,j\ldots)$ is associated with a set of translationally symmetric nets to generate the resulting structures.

Above, we saw that sheet-silicate arrangements containing single-layer and double-layer sheets may be generated from topologically planar 3-connected nets either [1] directly by associating high-valence cations with the vertices of such nets and T–O–T linkages with the edges of the nets, and [2] by combining [1] with oikodoméic operations to produce more topologically complicated structures. We will now look at the stoichiometric implications of these two processes.

The effect of net type on stoichiometry for single-layer sheets of tetrahedra

Consider the 3-connected tetrahedron shown in Fig. 33*a*. How many of these $TO_{2.5}$ units occur in the chemical formula depends first of all on the type of 3-connected net on which the sheet is based. Figure 7 shows the simpler nets of this type that we have considered above: $(6^3)_2$, $(4.8^2)_4$ and $(4.6.8)_4(6.8^2)_2$. The unit cells of these nets define the smallest possible unit of tetrahedra that are consistent with the arrangement of each net: $[T_2O_5]$, $[T_4O_{10}]$ and $[T_6O_{15}]$. The formula shown beneath each net is the simplest possible formula for that net; the arrows indicate that multiples of the formula given are possible in the direction of the arrow, associated with other topological characteristics of the sheet that enlarge the unit cell, such as different u-d arrangements in different rings, order of different types of cations at different tetrahedra, and arrangements of non-tetrahedrally coordinated cations that are inconsistent with the translational symmetry of the sheet of tetrahedra.

A formula-generating function for single-layer sheets of tetrahedra

The T:O ratio in a chemical formula depends on the relative numbers of differently connected vertices in the net on which the sheet is based. The different possible types of tetrahedra are listed in Table 3, and are associated with index numbers h to n that denote the numbers of each type of tetrahedron in the unit cell and the class of oikodoméic operator that produces the double-layer sheet. The arrows in Table 3 denote whether a tetrahedron points upwards or downwards (see Fig. 31), and the tetrahedron stoichiometry contributed to the resultant sheet is noted for single-layer ($N = 1$) and double-layer ($N = 2$) sheets.

As we will see below when we derive our formula-generating function for double-layer sheets, the class of the oikodoméic operator (2 or 3) affects the stoichiometry of double-layer sheets. However, if we wish to have a single formula-generating function for both type of sheets, the formula-generating function we derive for single-layer sheets must contain the connectivity information required by the formula-generating function for double-layer sheets.

Consider a single-layer sheet of tetrahedra with all tetrahedron connectivities listed in Table 3. This sheet will have the following stoichiometry: $(TO_3) \times (h + i + j) + (TO_{2.5}) \times (k + l + m) + (TO_2) \times n = T_{[h+i+j+k+l+m+n]}O_{[3(h+i+j)+2.5(k+l+m)+2n]}$. In single-layer sheets, the stoichiometry is unaffected by the u-d characteristics of the tetrahedra, and we may write our formula-generating function for single-layer sheets of tetrahedra as follows:

$$\begin{aligned} F_{[i,j,k,l,m,n]} &= F_{[(h+i+j),(k,l,m),n)]} \\ &= T_{[(h+i+j)+(k+l+m)+n]} \\ &\quad O_{[3(h+i+j)+2.5(k+l+m)+2n]} \end{aligned} \qquad [1]$$

where the individual indices are combined as

https://doi.org/10.1180/minmag.2015.079.7.17 Published online by Cambridge University Press

TABLE 3. Types of tetrahedra and their index number (h to n).

Tetrahedron type in parent net*	Number	Oikodoméic operation	$N=1$	$N=2$
2-connected ↑	h	Class 2	TO_3	TO_3
2-connected ↓	i	Class 2	TO_3	TO_2
2-connected ↓	j	Class 3	TO_3	TO_2
3-connected ↑	k	Class 2	$TO_{2.5}$	$TO_{2.5}$
3-connected ↓	l	Class 2	$TO_{2.5}$	TO_2
3-connected ↓	m	Class 3	$TO_{2.5}$	TO_2
4-connected	n	Class 2	TO_2	TO_2

*The arrows indicate u(↑) and d(↓) tetrahedra, respectively.

indicated because, as noted above, the u-d character of the tetrahedra do not affect the stoichiometry of single-layer sheets. This formula quantitatively expresses how the connectivities of tetrahedra within a sheet affect the stoichiometry of that sheet.

Some examples involving the 6^3 net

A very simple example has h = i = j = 0; k = 2; l = m = n = 0:

$$F_{[(0+0+0),(2,0,0),0)]} = T_{[(0+0+0)+(2+0+0)+0]} O_{[3x(0+0+0)+2.5x(2+0+0)+2\times0]} = [T_2O_5] = \text{the } \textbf{mica} \text{ sheet.}$$

Consider 2-connected and 3-connected tetrahedra with a unit cell equal to that of the parent $(6^3)_2$ net, where (h + i + j) = 2, (k + l + m) = 2 and n = 0 (i.e. there are two 2-connected tetrahedra and two 3-connected tetrahedra in the unit cell of the parent sheet; Fig. 18*a*):

$$F_{[(h+i+j),(k+l+m),n]} = F_{[(2),(2),0]} = T_{[(2)+(2)+0]} O_{[3\times(2)+2.5x(2)+2\times0]} = [T_4O_{11}]$$

which corresponds to the silicate sheet in **tumchaite**: $Na_2(Zr,Sn)[Si_4O_{11}](H_2O)_2$ (Subbotin *et al*., 2000).

Consider 2-connected and 3-connected tetrahedra with a unit cell equal to that of a parent $(6^3)_4$ net, where (h + i + j) = 3, (k + l + m) = 2 and n = 0:

$$F_{[(h+i+j),(k+l+m),n]} = F_{[(3),(2),0]} = T_{[(3)+(2)+0]} O_{[3\times(3)+2.5x(2)+2\times0]} = [T_5O_{14}]$$

which corresponds to the silicate sheet in **zeophyllite**: $Ca_{13}[Si_5O_{14}]_2F_8(OH)_2(H_2O)_6$, Z = 3 (six sheets per unit cell).

Consider 2-connected and 3-connected tetrahedra where the inserted 2-connected vertices are not *trans* in the six-membered ring (e.g. Fig. 14, arrangement [101000]). Because of the latter condition, the unit cell must be doubled relative to that of the $(6^3)_2$ net, i.e. the parent net is $(6^3)_4$ (Fig. 20*a*). Thus (h + i + j) = 2, (k + l + m) = 4, and n = 0:

$$F_{[(h+i+j),(k+l+m),n]} = F_{[(3),(2),0]} = T_{[(3)+(2)+0]} O_{[3x(3)+2.5\times(2)+2\times0]} = [T_5O_{14}]$$

which corresponds to the silicate sheet in **kvanfjeldite**: $Na_4(Ca,Mn)[Si_6O_{16}]$.

Some examples involving the 4^4 net

Consider 2-connected and 4-connected tetrahedra with a unit cell twice that of the $(4^4)_1$ net, i.e. the parent net is $(4^4)_2$ and the inserted net has (h + i + j) = 2, (k + l + m) = 0 and n = 2:

$$F_{[(h+i+j),(k+l+m),n]} = F_{[(2),(0),2]} = T_{[2+0+2]} O_{[3\times(2)+2.5\times(0)+2\times2]} = [T_4O_{10}]$$

which corresponds to the aluminosilicate sheet in **prehnite**: $Ca_2Al[AlSi_3O_{10}](OH)_2$ (Papike and Zoltai, 1967; Zunic *et al*., 1990; Baur *et al*., 1990).

Consider 3-connected and 4-connected tetrahedra with a unit cell four times that of the $(4^4)_1$ net,

https://doi.org/10.1180/minmag.2015.079.7.17 Published online by Cambridge University Press

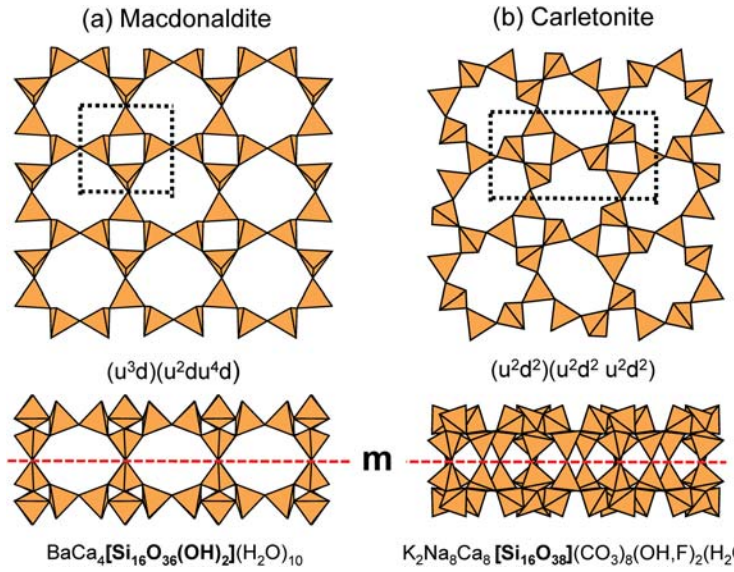

FIG. 34. The parent upper single-layer sheets and double-layer sheets in (*a*) **macdonaldite**, and (*b*) **carletonite**. The chemical compositions are shown in bold in the mineral formulae.

where (h + i + j) = 0, (k + l + m) = 8 and n = 4:

$$\begin{aligned} F_{[(h+i+j),(k+l+m),n]} &= F_{((0),(8),4)} \\ &= T_{(0+8+4)}O_{(3\times(0)+2.5\times(8)+2\times4)} \\ &= [T_{12}O_{28}] \end{aligned}$$

which corresponds to the beryllo-alumino-silicate sheet in **meliphanite**: $Ca_4(Na,Ca)_4[Be_4AlSi_7O_{24}(F,O)_4]$ (Dal Negro *et al.*, 1967; Grice and Hawthorne, 2002).

A formula-generating function for double-layer sheets of tetrahedra

We express the symbol for a double-layer sheet as the symbol for the corresponding single-layer sheet plus an associated oikodoméic operation. If this algebraic approach to formula generation is valid, we should be able to derive our formula-generating function for double-layer sheets from that for single-layer sheets.

To illustrate the effect of oikodoméic operations through connecting anions, consider the double-layer sheet in Fig. 31, in which k 3-connected tetrahedra in the upper single-layer sheet point upwards and l 3-connected tetrahedra in the upper single-layer sheet point downwards (per unit cell). The oikodoméic mirror operation doubles the number of atoms except for those that lie on the plane of the mirror itself, i.e. the apical anions of the d tetrahedra, which remain unchanged by the oikodoméic mirror operation (shown as green circles in Fig. 31). Thus when writing the formula-generating function for double-layer sheets, we must incorporate all different types of tetrahedra listed in Table 3, i.e. we do not now combine the indices indicating the number of u and d tetrahedra of the same connectedness as was the case for single-layer sheets. Thus we write the formula-generating function for single-layer sheets of 3-connected tetrahedra as:

$$\begin{aligned} F_{[h,i,j,k,l,m,n]} &= T_{[0+0+k+l+0+0]} \\ &\quad O_{[3\times0+3\times0+3\times0+2.5k+2.5l+2.5\times0+2\times0]} \\ &= T_{[k+l]}O_{[2.5(k+l)]}. \end{aligned}$$

This formula is doubled by the oikodoméic mirror operation except for l apical anions of the downward-pointing l tetrahedra that lie in the plane of the mirror operator: thus

$$F_{2[k,l]} = T_{[2(k+l)]}O_{[2\times2.5(k+l)-l]} = T_{[2(k+l)]}O_{[5k+4l]}.$$

Consider the sheets in **macdonaldite** (Cannillo *et al.*, 1968) and **carletonite** (Chao, 1972), based on the $(4.8^2)_n$ nets. The sheet in macdonaldite is based on the $(4.8^2)_4$ net (Fig. 34*a*) (i.e. with the minimal unit cell) for which k = 3 and l = 1. An

https://doi.org/10.1180/minmag.2015.079.7.17 Published online by Cambridge University Press

oikodoméic mirror operation through all apical anions of the d tetrahedra (Fig. 34) gives the formula-generating function:

$$F_{[3,1)} = T_{[2(3+1)]}O_{[2\times2.5(3+1)-1]} = [T_8O_{19}]$$

which is in accord with the sheet formula in **macdonaldite**: $BaCa_4[Si_8O_{18}(OH)]_2(H_2O)_{10}$ in which one apical anion is an (OH) group; note that there is only 0.5 Ba atom associated with the topological unit cell of the sheet, and thus the formula of the complete mineral is doubled to give an integer number of Ba atoms. We could also use the observed (structure) unit cell which is based on the $(4.8^2)_{16}$ net with k = 12 and l = 4:

$$F_{[3,1)} = T_{[2(12+4)]}O_{[2\times2.5(12+4)-4]} = [T_{32}O_{76}].$$

In the observed structure of macdonaldite, the unit cell actually contains two double-sheets (which we cannot predict at the present state of affairs) and hence the stoichiometry of the two double sheets is $2 \times [T_{32}O_{76}]$ which again is in accord with the formula of **macdonaldite**: $BaCa_4[Si_{16}O_{36}(OH)_2](H_2O)_{10}$ with $Z = 4$. In **carletonite**, the four-membered ring has the arrangement (u^2d^2), and cannot fit into the $(4.8^2)_4$ net, it can only fit into the $(4.8^2)_{16}$ net. Inspection of Fig. 34*b* shows that k = l = 8, and hence

$$F_{[8,8)} = T_{[2(8+8)]}O_{[2\times2.5(8+8)-8]} = [T_{32}O_{72}] = 4 \times [T_8O_{18}]$$

which is in accord with the sheet formula in **carletonite**: $KNa_4Ca_4[Si_8O_{18}](CO_3)_4(OH,F)(H_2O)$ with $Z = 4$. Thus comparison of **carletonite** and **macdonaldite** shows very clearly that the total number of anions in a double-layer sheet is affected by the u-d relations of the tetrahedra in the parent upper single-layer sheet.

The oikodoméic two-fold rotation operation, as in **naujakasite** (Fig. 28; Basso *et al*., 1975), has the same effect. The structure of the parent upper single-sheet is based on the $(6^3)_6$ net with four (u^2d^4) six-membered rings and two (ud^2ud^2) six-membered rings. Thus k = 2 and l = 4, and using the formula-generating function $F_{[k,l)} = T_{[2(k+l)]}O_{[2\times2.5(k+l)-l]}$ developed above specifically for double sheets with only 3-connected tetrahedra, we get

$$F_{[k,l)} = T_{[2(k+l)]}O_{[2\times2.5(k+l)-l]} = T_{[2(2+4)]}O_{[2\times2.5(2+4)-4]} = [T_{12}O_{26}]$$

which is in accord with the sheet formula in **naujakasite**: $Na_6(Fe^{2+},Mn^{2+})[Al_4Si_8O_{26}]$.

Oikodoméic operations through connecting anions change the tetrahedron connectivity from 3 to 4. We have used the indices j, l and m in Table 3 to identify the tetrahedra affected in this fashion by oikodoméic operations, and note that each change from 3-connected tetrahedra to 4-connected tetrahedra changes the stoichiometric contributions of 3-connected tetrahedra from $TO_{2.5}$ in single-layer sheets to 4-connected TO_2 in double-layer sheets (Table 3).

Oikodoméic mirror and two-fold-rotation operations through cations of d tetrahedra linking double-layer sheets (Figs 26*c*,*d*) replicate all u tetrahedra of the parent upper single-layer sheet in the lower single-layer sheet. However, this is not the case for the d tetrahedra; in both mirror and two-fold-rotation operations, the d tetrahedra are not replicated but their connectivity is modified from 3 to 4 (Table 3) in the resulting double-layer sheet.

Where there are incomplete oikodoméic mirror operations, the tetrahedra not replicated by this operation may be indicated by prime following the index number of the tetrahedron. Consider a parent upper-layer sheet of d tetrahedra based on the $(6^3)_2$ net. Inspection of Table 3 indicates that l = 2 for this net. However, if one of these tetrahedra is not replicated by the oikodoméic operation, then l = 2 and l′ = 1, denoting that there are two 3-connected d tetrahedra and that one of them is not replicated by the oikodoméic operation.

A formula-generating function for double-layer sheets of tetrahedra

From the above discussion, it is apparent that all h, i, k, l and n T cations are doubled in number by oikodoméic operations, whereas the j and m T cations are not doubled. Hence the number of T cations in a double-layer sheet is 2(h + i + k + l + n) + j + m. Now let us consider the anions in a double-layer sheet. From Table 3, we may write the number of anions as follows: $2 \times 3 \times h + 2 \times 2 \times i + 2 \times j + 2 \times 2.5 \times k + 2 \times 2 \times l + 2 \times m + 2 \times 2 \times n$), the first multiplier 2 resulting from the oikodoméic operation that produces the double-layer sheet; this expression simplifies to 6h + 4i + 5k + 4l + 4n + 2(j + m). We may thus write the formula-generating function for double-layer sheets of tetrahedra as follows:

$$F_{[h,i,j,k,l,m,n]} = T_{[2(h+i+k+l+n)+j+m]}O_{[6h+4i+5k+4l+4n+2(j+m)]}. \quad [2]$$

https://doi.org/10.1180/minmag.2015.079.7.17 Published online by Cambridge University Press

Incorporation of incomplete oikodoméic operations

Consider what happens where a tetrahedron in the upper-layer sheet is not replicated in the lower-layer sheet for a class-2 (e.g. Figs 26*a*,*b*) or a class-3 (e.g. Figs 26*c*,*d*) oikodoméic operation. The 2-connected anions of each k′ tetrahedron in the upper-layer sheet are still replicated in the lower-layer sheet as they also belong to other tetrahedra of the upper-layer sheet that are replicated in the lower-layer sheet, and the anion lying on the plane of the oikodoméic operation remains. Any non-apical 1-connected anions of each k′ tetrahedron in the upper-layer sheet are not replicated as they are not shared with any other tetrahedra. Thus the incomplete class-2 oikodoméic operation does not replicate the T cation, the apical anion and any 1-connected anions of the non-replicated upper-layer tetrahedron. Hence the T cation and any 1-connected anions of the non-replicated upper-layer tetrahedron must be subtracted from the formula for the double-layer sheet produced by the generating function.

Some examples

Consider 3-connected tetrahedra with a unit cell equal to that of the parent net $(3.8^2)_6(6.8^2)_6$ with a class-3 oikodoméic mirror operation through the central T cation of the d tetrahedra for k = m = 6 and h = i = j = l = n = 0:

$$\begin{aligned} F_{[(h+i+j),(k+l+m),n]} &= F_{[(2),(4),0]} \\ &= T_{[(2)+(4)+0]}O_{[3\times(2)+2.5\times(4)+2\times0]} \\ &= [T_6O_{16}] \end{aligned}$$

which corresponds to the silicate sheet in **zussmanite**, $K(Fe,Mg,Mn)_{13}[(Si,Al)_{18}O_{42}](OH)_{14}$ (Lopes-Vieira and Zussman, 1969).

Consider the net in Fig. 30*a*. This consists of a parent $(6^3)_2$ net (vertices shown in red) with pairs of 2-connected vertices (in blue and pink) inserted along four of the six edges of the parent net, resulting in a $(14^3)_{12}$ net. Inspection of the corresponding silicate sheet (Fig. 30*b*) shows that all 3-connected tetrahedra of the parent $(6^3)_2$ net point up (k = 4), the pink 2-connected tetrahedra point up (h = 4), and the blue 2-connected tetrahedra point down. There is an oikodoméic two-fold rotation operation through the central T cation of the tetrahedra shown in blue (Fig. 30*b*), and the 2-connected tetrahedra are of type j (Table 3). For h = j = 4, k = 4, i = l = m n = 0:

$$\begin{aligned} F_{[4,0,4,4,0,0,0)} &= T_{[2(4+0+4+0+0)+4+0]} \\ O_{[6\times4+5\times4+4\times0+4\times0+4\times0+2(4+0)]} &= [T_{20}O_{52}] \end{aligned}$$

which corresponds to the silicate sheet in **lemoynite**, $(Na,K)CaZr_2[Si_{10}O_{26}](H_2O)_{5\text{-}6}$ with $Z = 4$ (Blinov *et al*., 1975; LePage and Perrault, 1976), as there are two double-layer sheets in the unit cell.

Wickenburgite is a double-layer sheet-silicate mineral with the parent sheet based on the $(6^3)_6$ net with the tetrahedra in the arrangement (u^3dud). There is an incomplete oikodoméic operation: one tetrahedron in the upper parent single-layer sheet is not replicated by the oikodoméic operation (a two-fold rotation, class-2); this tetrahedron is shown in red in Figs 35*a*,*c* and is missing in the lower replicated single-layer sheet in Fig. 35*b*. The unit cell (Fig. 35*a*) of the parent single-layer sheet contains 4 u tetrahedra and 2 d tetrahedra, and 1 of the u tetrahedra is not replicated. Thus h = i = j = 0, k = 4, k′ = 1, l = 2, m = n = 0 (note that all u tetrahedra are counted by the index k, and the index k′ serves to denote those u tetrahedra that are not replicated). The generating function for double-layer sheet silicates, $F_{[h,i,j,k,l,m,n]} = T_{[2(h+i+k+l+n)+j+m]}O_{[6h+4i+5k+4l+4n+2(j+m)]}$ reduces to $F_{[0,0,0,k,l,0,0]} = T_{[2(0+0+k+l+0)+0+0]}O_{[6\times0+4\times0+5k+4l+4\times0+2(0+0)]} = T_{[2(k+l)]}O_{[5k+4l]}$. This must be modified by subtracting the T cations and apical anions of the k′ tetrahedra; thus

$$F_{[h,i,j,k,l,m,n]} = T_{[2(4+2)-1]}O_{[5\times4+4\times2-1]} = [T_{11}O_{27}]$$

which corresponds to the aluminosilicate sheet in **wickenburgite**, $Pb_3CaAl[AlSi_{10}O_{27}](H_2O)_4$ (Lam *et al*., 1994).

A single formula-generating function for single- and double-layer sheets of tetrahedra

As these formula-generating functions are algebraic in nature, we can manipulate them as such. Thus we should be able to combine the generating functions [1] and [2] for single-layer and double-layer sheets into a single function that will work for both types of sheet.

We will introduce the index variable N where $N = 1$ for single-layer sheets and $N = 2$ for double-layer sheets. We may then combine the left-hand-side of the formula-generating functions as $F_{N(i\ldots n)}$. The right-hand-side of the formula-generating functions may be produced by introducing N into the function such that equation [1] results for $N = 1$ and equation [2] results for $N = 2$. Some elementary

https://doi.org/10.1180/minmag.2015.079.7.17 Published online by Cambridge University Press

algebra gives the following function:

$$F_{[N(h+i+k+l+n)+j+m]} = T_{[N(h+i+k+l+n)+j+m]}$$
$$O_{[3Nh+(N+2)i+(4-N)j+2.5Nk+(1.5N+1)l+(3-0.5N)m+2Nn]}. \quad [3]$$

Some examples

Esquireite is a double-layer sheet silicate mineral with the parent sheet based on a $(6^3)_2$ net with two 2-connected vertices inserted *trans* to each other in every six-membered ring in the net (Figs 17*a*, 36*a*), and the relevant oikodoméic operation is a two-fold rotation (class-2). The 3-connected tetrahedra in the parent six-membered ring have the arrangement (ududud) and the inserted 2-connected vertices are both d (shown in yellow in Fig. 36*a*); thus in the unit cell of the parent sheet, h = 0, i = 1, j = 0, k = 1, l = 1, m = n = 0 (note that the unit cell shown in Fig. 36*a* is that of the structure; the unit cell of the net is actually half the unit cell shown, i.e. there are three vertices in the unit cell of the net):

$$F_{[2(0+1+1+1+0)+0+0]} = T_{[2(0+1+1+1+0)+0+0]}$$
$$O_{[3\times2\times0+(2+2)\times1+(4-2)\times0+2.5\times2\times1+(1.5\times2+1)\times1+(3-0.5\times2)\times0+2\times2\times0]}$$
$$= [T_6O_{13}]$$

which corresponds to the silicate sheet in **esquireite**, $Ba[Si_6O_{13}](H_2O)_7$ (Kampf *et al*., 2015).

Tuscanite is also a double-layer sheet-silicate mineral with the parent sheet based on a $(6^3)_4$ net with two 2-connected vertices inserted *trans* to each other in every other six-membered ring in the net (Fig. 36*b*), and the relevant oikodoméic operation is a two-fold screw-rotation (class-2). The 3-connected tetrahedra in the parent six-membered ring have the arrangement (d^6) and the inserted 2-connected vertices are both u; thus in the unit cell of the parent sheet, h = 1, i = 0, j = 0, k = 0, l = 4, m = n = 0:

$$F_{[2(1+0+0+2+0)+0+0]} = T_{[2(1+0+0+4+0)+0+0]}$$
$$O_{[3\times2\times1+(2+2)\times0+(4-2)\times0+2.5\times2\times0+(1.5\times2+1)\times4+(3-0.5\times2)\times0+2\times2\times0]}$$
$$= [T_{10}O_{22}]$$

which corresponds to the silicate sheet in **tuscanite**, $KCa_6[(Si,Al)_{10}O_{22}](SO_4,CO_3)_2(OH)(H_2O)$ (Mellini *et al*., 1977), and **latiumite**, $2\times(Ca,K)_4[(Si,Al)_5O_{11}](SO_4,CO_3)$ (Cannillo *et al*., 1973) in which the oikodoméic operation is a glide plane (class-2).

Bannisterite is a double-layer sheet-silicate mineral with the parent sheet based on the $(5.6^2)_8(5.6.7)_8(5.7^2)_4(6^2.7)_{12}$ net of 3-connected tetrahedra (Fig. 37*a*) with four distinct types of vertex, all of which are 3-connected. The relevant oikodoméic operation is a mirror (class-2) (Fig. 37*b*), and the unit cell (Fig. 37*b*) contains 24 u tetrahedra and 8 d tetrahedra. Thus h = i = j = 0, k = 24, l = 8, m = n = 0:

$$F_{[2(0+0+24+8+0)+0+0]} = T_{[2(0+0+24+8+0)+0+0]}$$
$$O_{[3\times2\times0+(2+2)\times0+(4-2)\times0+2.5\times2\times24+(1.5\times2+1)\times8+(3-0.5\times2)x0+2\times2\times0]}$$
$$= [T_{64}O_{152}]$$

which corresponds to the silicate sheet in bannisterite, $4\times(Ca,K,Na)(Mn^{2+},Fe^{2+})_{10}[(Si,Al)_{16}O_{38}](OH)_8(H_2O)$, Heaney *et al*., (1992). Note that in **bannisterite**, $Z = 8$, but there are two double-layer sheets in the unit cell.

Diegogattaite, $Na_2CaCu_2[Si_8O_{20}](H_2O)$ (Rumsey *et al*., 2013; Welch and Rumsey, 2013) is a double-layer sheet-silicate mineral with a parent single-layer net (Fig. 38*a*) that at first sight seems rather complicated, with both 2-connected and 3-connected vertices. If we delete the 2-connected vertices from the net, we see that the parent net is actually 4.8^2 (Fig. 38*b*). If we insert a pair of 2-connected vertices into one edge of the four-membered ring and a single 2-connected vertex into each edge between two eight-membered rings (Fig. 38*c*), the one-layer net of **diegogattaite** (Fig. 38*a*) is the result. However, the net of Fig. 38*a* may be derived in a much more simple fashion from the 6^3 net by a different operation. Selected edges may be deleted from the 6^3 net to produce the net of Fig. 38*a*; as shown in Fig. 39*a*,*c*, deletion of the dotted edges of the 6^3 net leads directly to the diegogattaite net (Fig. 38*a*) and its corresponding sheet (Fig. 39*b*). The cross-section of the parent upper-layer sheet (Fig. 39*d*) contains both u and d tetrahedra, and the double-layer sheet (Fig. 39*e*) is derived by the oikodoméic operation shown in Fig. 26*b*. The unit cell of the parent upper layer sheet contains eight 2-connected tetrahedra and eight 3-connected tetrahedra. The 2-connected tetrahedra face upwards and hence h = 8, and the 3-connected tetrahedra face downwards, and hence l = 8. Thus for $N = 2$, h = l = 8, i = j = k = m = n = 0:

$$F_{[2(8+0+0+8+0)+0+0]} = T_{[2(8+0+0+8+0)+0+0]}$$
$$O_{[3\times2\times8+(2+2)0+(4-2)0+2.5\times2\times0+(1.5\times2+1)8+(3-0.52)0+2\times2\times0]}$$
$$= [T_{32}O_{80}].$$

https://doi.org/10.1180/minmag.2015.079.7.17 Published online by Cambridge University Press

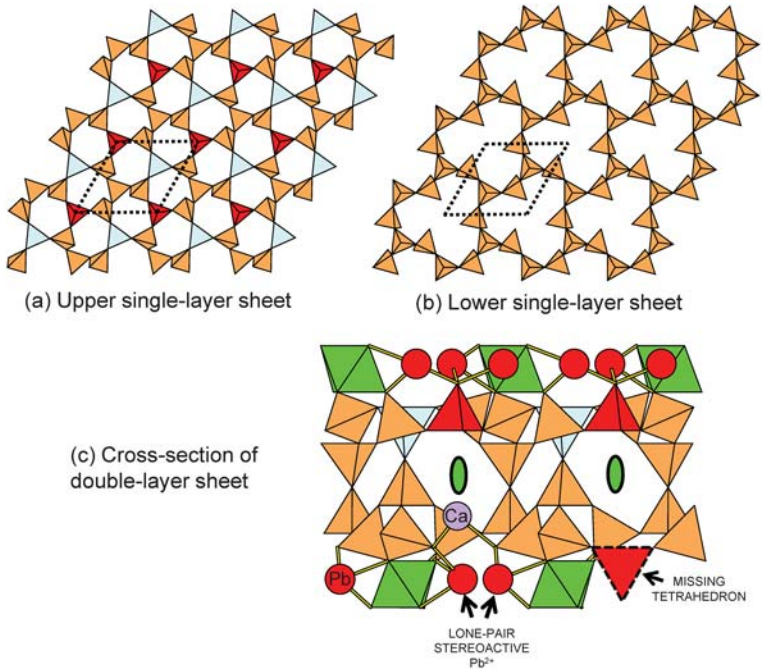

FIG. 35. The tetrahedron sheet in **wickenburgite**; (*a*, *b*) the upper parent single-layer sheet and the partly replicated lower single-layer sheet; (*c*) cross-section of the double-layer sheet. Legend as in Fig. 1, plus blue: Al tetrahedra; red: tetrahedra that are not replicated by the oikodoméic two-fold-rotation operator (shown as green lozenges); the red tetrahedron with dashed edges shows the position where the red tetrahedron would occur if it were replicated; lilac circle: Ca; red circle: lone-pair stereoactive Pb^{2+} 'replacing' the missing red tetrahedron.

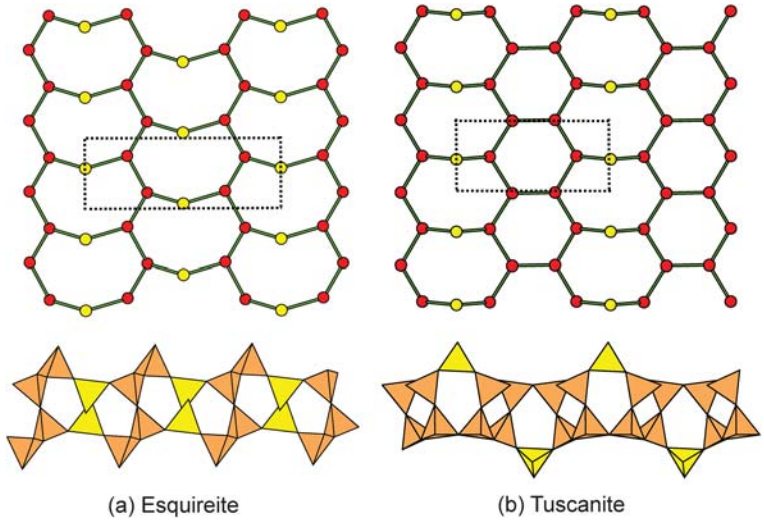

FIG. 36. The parent upper single-layer sheets and cross-sections of the double-layer sheets in (*a*) **esquireite**, and (*b*) **tuscanite**. The yellow vertices represent the inserted 2-connected vertices in the parent upper single-layer nets and the yellow tetrahedra are the inserted 2-connected tetrahedra in the double-layer sheets.

https://doi.org/10.1180/minmag.2015.079.7.17 Published online by Cambridge University Press

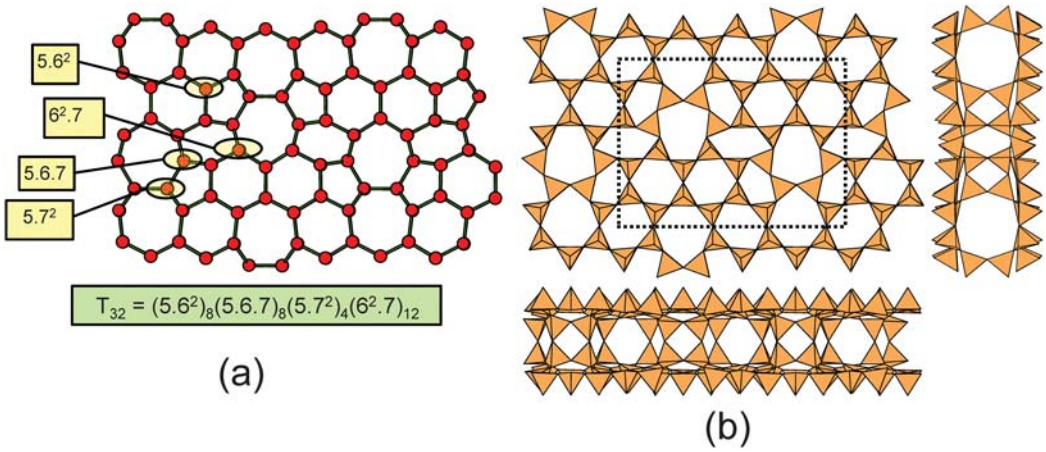

FIG. 37. The tetrahedron sheet in **bannisterite**; (*a*) the 3-connected parent $(5.6^2)_8(5.6.7)_8(5.7^2)_4(6^2.7)_{12}$ net, with the various types of vertices shown; (*b*) plan view and horizontal views of the complete double-layer sheet.

The formula of **diegogattaite** is $Na_2CaCu_2[Si_8O_{20}](H_2O)$ with $Z = 4$; thus the unit cell contains $[Si_8O_{20}] \times 4 = [Si_{32}O_{80}] = [T_{32}O_{80}]$ in accord with the above calculation.

Structure-generating functions

The formula-generating functions derived above are independent of the type of net on which the

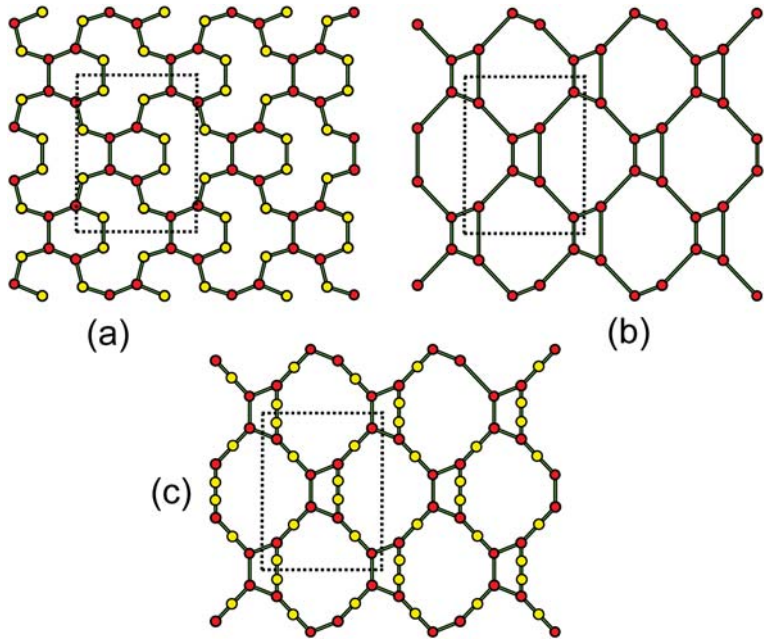

FIG. 38. (*a*) The net of Si atoms in **diegogattaite**; (*b*) the net in (*a*) with the 2-connected Si atoms (= vertices) removed, showing that the 3-connected vertices form a 4.8^2 net; (*c*) insertion of 2-connected vertices into selected edges of the 4.8^2 net in (*b*), producing a net that is topologically identical to the **diegogattaite** net in (*a*). Legend as in Fig. 1, 2-connected vertices are indicated by yellow circles.

https://doi.org/10.1180/minmag.2015.079.7.17 Published online by Cambridge University Press

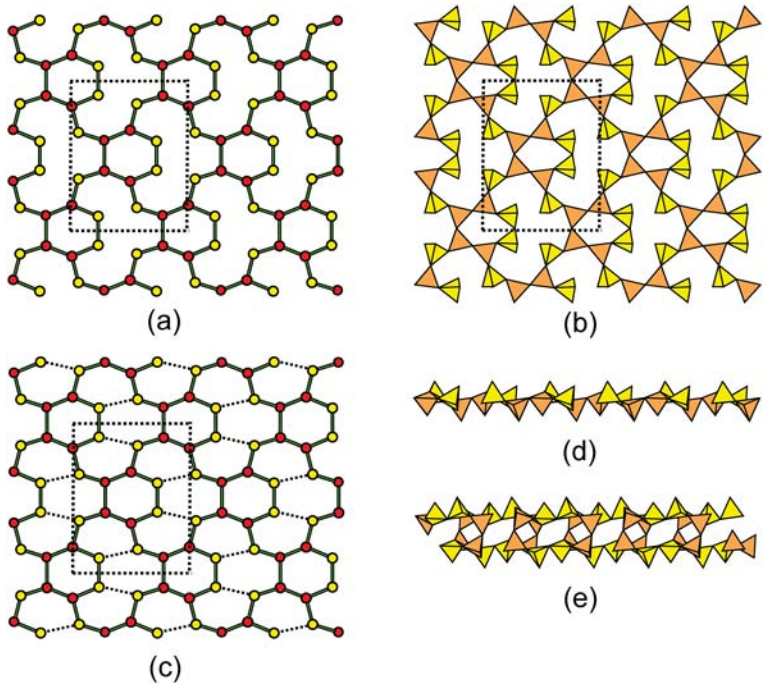

FIG. 39. (*a*) The net in **diegogattaite**; (*b*) the upper-layer sheet of tetrahedra in **diegogattaite**; (*c*) the 6^3 net, showing the edges (dotted lines) that must be deleted to form the net in (*a*); (*d*) the upper-layer sheet in **diegogattaite** viewed in cross-section; (*e*) the double-layer sheet of tetrahedra in **diegogattaite** viewed in cross-section. 3-connected tetrahedra are brown, 2-connected tetrahedra are yellow.

structure is based; the only important characteristic of the net is the number of vertices in the unit cell. However, if we associate formula-generating function [3] with a specific net, we can generate the bond topology of the sheet of tetrahedra in a straightforward manner. We may denote this as follows:

$$\mathrm{D{:}F}_{[N(\mathrm{h+i+k+l+n})+\mathrm{j+m}]} = \mathrm{T}_{[N(\mathrm{h+i+k+l+n})+\mathrm{j+m}]}$$
$$\mathrm{O}_{[3N\mathrm{h}+(N+2)i+(4-N)\mathrm{j}+2.5N\mathrm{k}+(1.5N+1)\mathrm{l}+(3-0.5N)\mathrm{m}+2N\mathrm{n}]}$$

where D is the net that is combined with the formula-generating function to produce a structure. For example, consider the net $(5^2.8)_4(5.8^2)_2$ (Fig. 3*b*):

$$(5^2.8)_4(5.8^2)_2{:}\mathrm{F}_{[N(\mathrm{h+i+k+l+n})+\mathrm{j+m}]}$$
$$= \mathrm{T}_{[N(\mathrm{h+i+k+l+n})+\mathrm{j+m}]}$$
$$\mathrm{O}_{[3N\mathrm{h}+(\mathrm{N+2})\mathrm{i}+(4-\mathrm{N})\mathrm{j}+2.5\mathrm{Nk}+(1.5N+1)\mathrm{l}+(3-0.5N)\mathrm{m}+2N\mathrm{n}]}.$$

Let us insert 2-connected vertices along the edges connecting adjacent eight-membered rings as shown in Fig. 40*a*. The result is the structure illustrated in Fig. 40*b*. In the unit cell, there are the following types and numbers of tetrahedra: h = 1, i = j = m = n = 0, k = 4, l = 2.

$$\mathrm{F}_{[1(1+0+4+2+0)+0+0]} = \mathrm{T}_{[1(1+0+4+2+0)+0+0]}$$
$$\mathrm{O}_{[3\mathrm{h}+2.5\mathrm{k}+2.5\mathrm{l}]}$$

and thus the single-layer structure in Fig. 40*b* has the formula $[T_7O_{18}]$.

Let us now introduce a class-2 oikodoméic mirror operation as shown in Fig. 40*c*. In the unit cell of the parent upper-layer sheet, h = 1, i = j = m = n = 0, k = 4, l = 2 as before. However, $N = 2$ in the structure-generating function:

$$(5^2.8)_4(5.8^2)_2{:}\ \mathrm{F}_{[2(1+0+4+2+0)+0+0]}$$
$$= \mathrm{T}_{[2(1+0+4+2+0)+0+0]}\mathrm{O}_{[3\times2\times1+2.5\times2\times4+(1.5\times2+1)2]}$$

and thus the double-layer structure in Fig. 40*c* has the formula $[T_{14}O_{34}]$. Thus we may use the structure-generating function given above for single-layer and double-layer sheet-silicates to

https://doi.org/10.1180/minmag.2015.079.7.17 Published online by Cambridge University Press

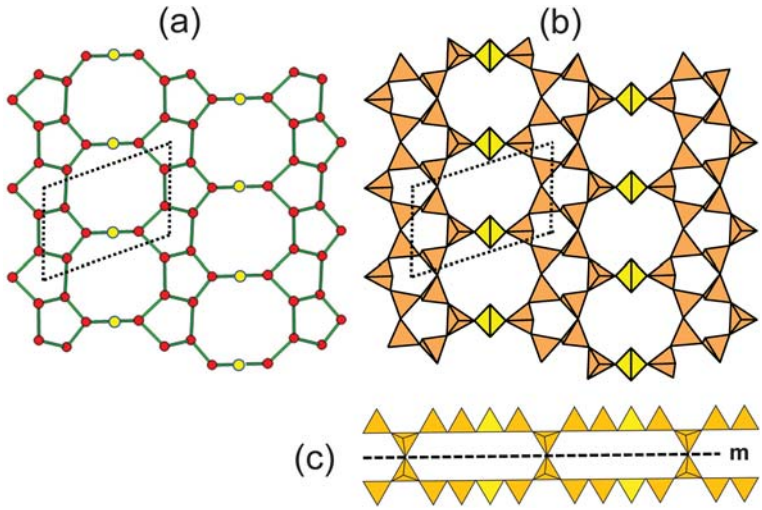

FIG. 40. (*a*) The $(5^2.8)_4(5.8^2)_2$ parent net with 2-connected vertices inserted along the edges adjacent to two eight-membered rings in the parent net; (*b*) the single-layer sheet of tetrahedra corresponding to the net in Fig. 40*a*; (*c*) a class-2 oikodoméic mirror operation replicating the upper single-layer and melding the two layers together to produce a double-layer sheet. Legend as in Figs 1 and 14.

derive the structure topology and stoichiometry of all such structures by combining 3-connected plane nets with different combinations of u-d tetrahedra and oikodoméic operations.

Summary

[1] Two-dimensional topologically planar nets may be used to examine the structure and stoichiometry of single-layer and double-layer sheet-silicate minerals (with tetrahedrally coordinated cations T = Si^{4+}, Al^{3+}, Fe^{3+}, B^{3+}, Be^{2+}, Zn^{2+} and Mg^{2+}).

[2] Many sheet-silicate minerals are based on the 3-connected plane nets 6^3, 4.8^2, $(4.6.8)_2(6.8^2)_1$ and $(5^2.8)_1(5.8^2)_1$, and a few more complicated nets have one or two representative structures, e.g. $(5.6.7)_4(5.7^2)_1(6^2.7)_1$, $(4.12^2)_2(4^2.12)_1$, $(5^2.8)_1(5.6^2)_1$ $(5.6.8)_2(6^2.8)_1$.

[3] Many of the more complicated minerals are based on sheets of 2-, 3- and 4-connected tetrahedra that may be developed from 3- and 4-connected plane nets by a series of oikodoméic operations on 3- or 4-connected nets that change the topology of the parent net.

[4] Insertion of 2-connected vertices into 3-connected plane nets gives rise to a series of single-layer minerals, e.g. **kvanfeldite**, **tumchaite**, **zeophyllite**.

[5] Insertion of 2- and 3-connected vertices into 4-connected plane nets gives rise to single-layer minerals, e.g. **prehnite**, **meliphanite**.

[6] Oikodoméic mirror and two-fold-rotation operators produce double-layer structures from parent single-layer structures, e.g. **dmisteinbergite** from the 6^3 net, **carletonite**, **macdonaldite** from the 4.8^2 net.

[7] We may incorporate aspects of the bond topology and chemical composition of single-layer and double-layer silicate minerals into a general expression that includes the stoichiometry and local topological details of the environment of each tetrahedron (the formula-generating function) that may be associated with a topologically two-dimensional net to form the structure-generating function that can generate both the formula and aspects of the structure of single-layer and double-layer silicates.

[8] Using these functions, we may generate formulae and structural arrangements of single-layer and double-layer silicate structures with specific local and long-range topological features.

Acknowledgements

The author thanks Mark Welch for his review of the paper. The work was funded by a Canada Research Chair in Crystallography and Mineralogy and by a

https://doi.org/10.1180/minmag.2015.079.7.17 Published online by Cambridge University Press

Discovery Grant from the Natural Sciences and Engineering Research Council of Canada.

References

Bakakin, V.V., Belov, N.V., Borisov S.V. and Solov'eva L. P. (1970) The crystal structure of nordite and its relationship to melilite and datolite-gadolinite. *American Mineralogist*, **55**, 1167–1181.

Basso, R., Dal Negro, A., Della Giusta, A. and Ungaretti, L. (1975) The crystal structure of naujakasite, a double sheet silicate. *Bulletin Grønlands Geologiske Indersøgelse*, **116**, 11–24.

Baur, W.H., Joswig, W., Kassner, D. and Hofmeister, W. (1990) Prehnite: structural similarity of the monoclinic and orthorhombic polymorphs and their Si/Al ordering. *Journal of Solid State Chemistry*, **86**, 330–333.

Blinov, V.A., Voronkov, A.A., Ilyukhin, V.V. and Belov, N.V. (1975) Crystal structure of lemoynite with a new type of mixed framework. *Soviet Physics Doklady*, **19**, 397–398.

Brualdi, R.A. (1977) *Introductory Combinatorics.* Elsevier Science, New York.

Cámara, F., Sokolova, E., Hawthorne, F.C., Rowe, R., Grice, J.D. and Tait, K.T. (2013) Veblenite, $K_2O_2Na(Fe^{2+}_5Fe^{3+}_4Mn_7O)Nb_3Ti(Si_2O_7)_2(Si_8O_{22})_2O_6(OH)_{10}(H_2O)_3$, a new mineral from Seal Lake, Newfoundland and Labrador: mineral description, crystal structure, and a new veblenite (Si_8O_{22}) ribbon. *Mineralogical Magazine*, **77**, 2955–2974.

Cannillo, E., Rossi, G., Ungaretti, L. and Carobbi, S.G. (1968) The crystal structure of macdonaldite. *Atti della Accademia Nazionale dei Lincei, Classe di Scienze Fisiche, Matematiche e Naturali, Rendiconti, Serie 8*, **45**, 399–414.

Cannillo, E., Dal Negro, A. and Rossi, G. (1973) The crystal structure of latiumite, a new type of sheet silicate. *American Mineralogist*, **58**, 466–470.

Capitani, G.C. and Mellini, M. (2006) The crystal structure of a second antigorite polysome (m = 16), by single-crystal synchrotron diffraction. *American Mineralogist*, **91**, 394–399.

Chakhmouradian, A.R., Cooper, M.A., Ball, N.A., Reguir, E.P., Medici, L., Abdu, Y.A. and Antonov, A.A. (2014) Vladykinite, $Na_3Sr_4(Fe^{2+}Fe^{3+})Si_8O_{24}$: A new complex sheet silicate from peralkaline rocks of the Murun complex, eastern Siberia, Russia. *American Mineralogist*, **99**, 235–241.

Chao, G.Y. (1972) The crystal structure of carletonite, $KNa_4Ca_4Si_8O_{18}(CO_3)_4F_{0.5}(OH)_{0.5}H_2O$, a double-sheet silicate. *American Mineralogist*, **57**, 765–778.

Chesnokov, B.V., Lotova, E.V., Nigmatulina, E.N., Pavlyuchenko, V.S. and Bushmakin, A.F. (1990) Dmisteinbergite $CaAl_2Si_2O_8$ (hexagonal) - a new mineral. *Zapiski Vsesoyuznogo Mineralogicheskogo Obshchestva*, **119**, 43–45 [in Russian].

Chukanov, N.V., Rastsvetaeva, R.K., Aksenov, S.M., Pekov, I.V., Zubkova, N.V., Britvin, S.N., Belakovskiy, D.I. and Ternes, B. (2012) Günterblassite, $(K,Ca)_{3-x}Fe[(Si,Al)_{13}O_{25}(OH,O)_4].7(H_2O)_7$, a new mineral: the first phyllosilicate with triple tetrahedral layer. *Geology of Ore Deposits*, **54**, 656–662.

Chukanov, N.V., Zubkova, N.V., Pekov, I.V., Belakovskiy, D.I., Schüller, W., Ternese, B., Blass, G. and Pushcharovsky, D.Yu. (2013) Hillesheimite, $(K,Ca,O)_2(Mg,Fe,Ca,O)_2[(Si,Al)_{13}O_{23}(OH)_6](OH).8H_2O$, a new phyllosilicate mineral of the günterblassite group. *Geology of Ore Deposits*, **55**, 549–557.

Cohen, D.I.A. (1978) *Basic Techniques in Combinatorial Theory.* John Wiley and Sons, New York.

Dal Negro, A., Rossi, G. and Ungaretti, L. (1967) The crystal structure of meliphanite. *Acta Crystallographica*, **23**, 260–264.

Ferraris, G., Khomyakov, A.P., Belluso, E. and Soboleva, S.V. (1998) Kalifersite, a new alkaline silicate from Kola Peninsula (Russia) based on a palygorskite-sepiolte poysomatic series. *European Journal of Mineralogy*, **10**, 865–874.

Garvie, L.A.J., Devouard, B., Groy, T.L., Cámara, F. and Buseck, P.R. (1999): Crystal structure of kanemite, $NaHSi_2O_5{\cdot}3H_2O$, from the Aris phonolite, Namibia. *American Mineralogist*, **84**, 1170–1175.

Giustetto, R. and Chiari, C. (2004) Crystal structure refinement of palygorskite from neutron powder diffraction. *European Journal of Mineralogy*, **16**, 521–532.

Grice, J.D. and Hawthorne, F.C. (2002) New data on meliphanite, $Ca_4(Na,Ca)_4Be_4AlSi_7O_{24}(F,O)_4$. *The Canadian Mineralogist*, **40**, 971–980.

Grice, J.D., Rowe, R., Poirier, G., Pratt, A. and Francis, J. (2009) Bussyite-(Ce), a new beryllium silicate mineral species from Mont Saint-Hilaire, Quebec. *The Canadian Mineralogist*, **47**, 193–204.

Hawthorne, F.C. (1983) Graphical enumeration of polyhedral clusters. *Acta Crystallographica* **A39**, 724–736.

Hawthorne, F.C. (2012) Bond topology and structure-generating functions: Graph-theoretic prediction of chemical composition and structure in polysomatic T–O–T (biopyribole) and H–O–H structures. *Mineralogical Magazine*, **76**, 1053–1080.

Hawthorne, F.C. and Smith, J.V. (1986*a*) Enumeration of 4-connected 3-dimensional nets and classification of framework silicates. 3-D nets based on insertion of 2-connected vertices onto 3-connected plane nets. *Zeitschrift für Kristallographie*, **175**, 15–30.

Hawthorne, F.C. and Smith, J.V. (1986*b*) Enumeration of 4-connected 3-dimensional nets and classification of framework silicates. Body-centred cubic nets based on the rhombicuboctahedron. *The Canadian Mineralogist*, **24**, 643–648.

Hawthorne, F.C. and Smith, J.V. (1988) Enumeration of 4-connected 3-dimensional nets and classification of

https://doi.org/10.1180/minmag.2015.079.7.17 Published online by Cambridge University Press

framework silicates. Combination of zigzag and saw chains with 6^3, 3.12^2, 4.8^2, 4.6.12 and $(5^2.8)_2(5.8^2)_1$ nets. *Zeitschrift für Kristallographie*, **183**, 213–231.

Hawthorne, F.C., Krivovichev, S.V. and Burns, P.C. (2000) The crystal chemistry of sulfate minerals. Pp. 1–112 in: *Sulfate Minerals: Crystallography, Geochemistry, and Environmental Significance* (C.N. Alpers, J.L. Jambor and D.K. Nordstrom, editors). Reviews in Mineralogy and Geochemistry, **40**. Mineralogical Society of America and the Geochemistry society, Washington, DC.

Heaney, P.J., Post, J.E. and Evans, H.T. Jr. (1992) The crystal structure of bannisterite. *Clays and Clay Minerals*, **40**, 129–144.

Johnsen, O., Leonardsen, E.S., Faelth, L. and Annehed, H. (1983) Crystal structure of kvanefjeldite: The introduction of $2(Si_3O_7OH)$ layers with eight-membered rings. *Neues Jahrbuch für Mineralogie Monatshefte*, **1983**, 505–512.

Kampf, A.R., Housley, R.M., Dunning, G.E. and Walstrom, R.E. (2015) Esquireite, BaSi6O13·7H2O, a new layer silicate from the barium silicate deposits of California. *The Canadian Mineralogist*, DOI:10.3749/canmin.1400076

Krivovichev, S.V. (2008) *Structural Crystallography of Inorganic Oxysalts.* International Union of Crystallography Monographs on Crystallography **22**, Oxford University Press.

Krivovichev, S.V. (2009) *Structural Mineralogy and Inorganic Crystal Chemistry.* St. Petersburg University Press, St. Petersburg, Russia, 398 pp.

Lam, A.E., Groat, L.A., Cooper, M.A. and Hawthorne, F. C. (1994) The crystal structure of wickenburgite, $Pb_3CaAl[AlSi_{10}O_{27}](H_2O)_3$, a sheet structure. *The Canadian Mineralogist*, **32**, 525–532.

Le Page, Y. and Perrault, G. (1976) Structure crystalline de la lemoynite, $(Na,K)_2CaZr_2Si_{10}O_{26}$,5-6$(H_2O)$. *The Canadian Mineralogist*, **14**, 132–138.

Liebau, F. (1985). *Structural Chemistry of Silicates.* Springer-Verlag, Berlin.

Lopes-Vieira, A. and Zussman, J. (1969) Further detail on the crystal structure of zussmanite. *Mineralogical Magazine*, **37**, 49–60.

Mazzi, F., Ungaretti, L. and Dal Negro, A. (1979) The crystal structure of semenovite. *American Mineralogist*, **64**, 202–210.

Mellini, M., Merlino, S. and Rossi, G. (1977) The crystal structure of tuscanite. *American Mineralogist*, **62**, 1114–1120.

Merlino, S. (1972) The crystal structure of zeophyllite. *Acta Crystallographica*, **B28**, 2726–2732.

Merlino, S. (1988) Gyrolite: its crystal structure and crystal chemistry. *Mineralogical Magazine*, **52**, 377–387.

Mikenda, W., Pertlik, F., Povondra, P. and Ulrych, J. (1997) On zeophyllite from Radejčín, České středohoří Mts.: X-ray and IR-investigations. *Mineralogy and Petrology*, **61**, 199–209.

Papike, J.J. and Zoltai, T. (1967) Ordering of tetrahedral aluminum in prehnite, $Ca_2(Al,Fe^{3+})[Si_3AlO_{10}](OH)_2$. *American Mineralogist*, **52**, 974–984.

Post, J.E., Bish, D.L. and Heaney, P.J. (2007) Synchrotron powder X-ray diffraction study of the structure and dehydration behavior of sepiolite. *American Mineralogist*, **92**, 91–97.

Quint, R. (1987) Description and crystal structure of amstallite, $CaAl(OH)_2[Al_{0.8}Si_{3.2}O_8(OH)_2]\cdot[(H_2O)_{0.8}Cl_{0.2}]$, a new mineral from Amstall, Austria. *Neues Jahrbuch für Mineralogie, Monatshefte*, **1987**, 253–262.

Rastsvetaeva, R.K., Aksenov, S.M. and Chukanov, N.V. (2012) Crystal structure of günterblassite, a new mineral with a triple layer. *Doklady Chemistry*, **442**, 57–62.

Rumsey, M.S., Welch, M.D., Kampf, A.R. and Spratt, J. (2013) Diegogattaite, $Na_2CaCu_2Si_8O_{20}\cdot H_2O$: a new nanoporous copper sheet silicate from Wessels Mine, Kalahari Manganese Fields, Republic of South Africa. *Mineralogical Magazine*, **77**, 3155–3162.

Sharygin, V.V., Pekov, I.V., Zubkova, N.V., Khomyakov, A.P., Stoppa, F. and Pushcharovsky, D.Yu. (2013) Umbrianite, $K_7Na_2Ca_2[Al_3Si_{10}O_{29}]F_2Cl_2$, a new mineral species from melilitolite of the Pian di Celle volcano, Umbria, Italy. *European Journal of Mineralogy*, **25**, 655–669.

Smith, J.V. (1977) Enumeration of 4-connected 3-dimensional nets and classification of framework silicates; I, Perpendicular linkage from simple hexagonal net. *American Mineralogist*, **62**, 703–709.

Smith, J.V. (1978) Enumeration of 4-connected 3-dimensional nets and classification of framework silicates, II, Perpendicular and near-perpendicular linkages from 4.8^2, 3.12^2 and 4.6.12 nets. *American Mineralogist*, **63**, 960–969.

Smith, J.V. (1988) Topochemistry of zeolites and related materials. I. Topology and geometry. *Chemical Reviews*, **188**, 149–182.

Subbotin, V.V., Merlino, S., Pushcharovskii, D.Yu Pakhomovskii, Y.A., Ferro, O., Bogdanova, A.V., Voloshin, A.V., Sorokhtina, N.V., Zubkova, N.V. (2000) Tumchaite $Na_2(Zr,Sn)Si_4O_{11}\cdot 2(H_2O)$ – a new mineral from carbonatites of the Vuoriyarvi alkali-ultrabasic massif, Murmansk region, Russia. *American Mineralogist*, **85**, 1516–1520.

Takeuchi, Y. and Donnay, G. (1959) The crystal structure of hexagonal $CaAl_2Si_2O_8$. *Acta Crystallographica*, **12**, 465–470.

Welch, M.D. and Rumsey, M.S. (2013) A new naturally-occurring nanoporous copper sheet-silicate with 6^48^2 cages related to synthetic "CuSH" phases. *Journal of Solid State Chemistry*, **203**, 260–265.

Zunic, T.B., Scavnicar, S. and Molin, G. (1990) Crystal structure of prehnite from Komiza. *European Journal of Mineralogy*, **2**, 731–734.